SUBSURFACE TRANSPORT OF PHOSPHORUS IN RIPARIAN FLOODPLAINS: TRACER AND PHOSPHORUS TRANSPORT EXPERIMENTS

By

JOHN WILLIAM FUCHS

Bachelor of Science in Civil Engineering

University of Mississippi

Oxford, MS

2006

Submitted to the Faculty of the
Graduate College of the
Oklahoma State University
in partial fulfillment of
the requirements for
the Degree of
MASTER OF SCIENCE
May 2008

SUBSURFACE TRANSPORT OF PHOSPHORUS IN RIPARIAN FLOODPLAINS: TRACER AND PHOSPHORUS TRANSPORT EXPERIMENTS

Thesis Approved:

Dr. Garey Fox
Thesis Adviser

Dr. Dan Storm

Dr. Glenn Brown

Dr. Chad Penn

Dr. A. Gordon Emslie
Dean of the Graduate College

PREFACE/ACKNOWLEDGEMENTS

I would like to thank a few people who were involved in this research. Without them, none of this work would have been possible. Mom, Dad, and Garth, thank you for all of your care and support throughout my life. I attribute everything positive that has happened for me so far directly to your encouragement. Dr. Fox, thank you for all of the opportunities and advice you have given me in the past 4 years. It has been an invaluable experience and I am a better person because of it. Your patience and tutelage towards me has made a lasting impression and I consider myself privileged to have had you as an advisor. Thank you to my committee members, Dr. Chad Penn, Dr. Dan Storm, and Dr. Glenn Brown, for all of your advice and help with field experiments and laboratory work. Also, thank you to Dr. Onur Akay, Jorge Guzman, Lisa Fultz, Mike Sample, and Audrey Sima for your help with the field work. It was no small task enduring the 100-degree heat, not to mention constantly fighting off ticks and mosquitoes. Without you all, this project would not have been completed.

TABLE OF CONTENTS

LIST OF TABLES

LIST OF FIGURES

Figure Page

Figure Page

CHAPTER I

INTRODUCTION

The impact of increased nutrient loadings on surface waters has drawn considerable attention in recent years. Polluted drinking water, excessive algal growth, taste and odor issues, and fish kills are only a few of the negative effects that can result from an overload of nutrients. As an example, Lakes Eucha and Spavinaw on Spavinaw Creek in northeast Oklahoma supply more than half of the drinking water for the cities of metropolitan Tulsa, Oklahoma. Due to the overabundance of nutrient loading in the watershed, excess growth of algae has degraded the water quality of the lake. The cost of drinking water treatment and the taste and odor problems have increased significantly in the past decade. While nitrogen is a concern, phosphorous (P) is generally considered the most limiting nutrient. The majority of P loading to the lake in this area comes from surface-applied poultry litter. Of the 48,000 kg/yr of phosphorous entering Lake Eucha, 69% is thought to come from poultry litter application as fertilizer to pasture and crops in the watershed (Wagner and Woodruff, 1997; Storm et al., 2001, 2002). Poultry is the principal industry in the basin. In the watershed, over 2,000 poultry houses produce approximately 91,700 tons of poultry litter each year, most of which is applied to permanent pastures.

P is an essential nutrient not only for crops but also for aquatic life. However, excessive soil P concentrations can increase potential P transport to surface waters or leaching into the subsurface. This can have serious negative implications. Daniel et al. (1998) found that concentrations of P critical for terrestrial plant growth were an order of magnitude larger than concentrations at which lake eutrophication may occur.

With these negative impacts in mind, researchers have investigated the sources of P loads reaching surface waters. Many studies found that the primary transport mechanism for P from the source to the water body occurred through surface transport (i.e. runoff of dissolved P or erosion of soil containing particulate P) and considered the role of subsurface transport to be negligible. However, there is a lack of research pertaining to the role of subsurface transport, especially in riparian floodplains. Riparian floodplains commonly consist of alluvial deposits that possess hydraulic properties conducive to the subsurface transport of P. This research attempts to quantify the role that a subsurface alluvial system can have in transporting P in a riparian floodplain.

CHAPTER II

REVIEW OF LITERATURE

2.1 Subsurface Nutrient Transport Studies

Subsurface P transport is a less studied and understood transport mechanism compared to transport by overland flow, although numerous studies have reported its occurrence (Andersen and Kronvang, 2006; Hively et al., 2006; Nelson et al., 2005; Kleinman et al., 2004). For example, Andersen and Krovang (2006) modified a P Index to incorporate potential P transport pathways of tile drains and leaching in Denmark. Hively et al. (2006) considered transport of total dissolved P (TDP) for both baseflow and surface runoff. Nelson et al. (2005) indicated that phosphorus leaching and subsurface transport should be considered when assessing long-term risk of P loss from waste-amended soils. Kleinman et al. (2004) noted that the P leaching is a significant, but temporally and spatially variable transport pathway. From research on four grassland soils, Turner and Haygarth (2000) documented that subsurface P transfer, primarily in the dissolved form, can occur at concentrations that could cause eutrophication. Other researchers are beginning to emphasize colloidal P transport in the subsurface, as P attaches to small size particles capable of being transported through the soil pore spaces (Heathwaite et al., 2005; Ilg et al., 2005; de Jonge et al., 2004).

Surface water problems resulting from excess nutrients is not a new issue. It has been studied for quite some time and researchers have developed management practices in an effort to reduce the nutrient loads associated with surface runoff. One of these management practices involves the use of vegetated buffer strips (VBS) along riparian areas. The VBS can be either grass or forested, and act as a zone in which runoff is captured and sediment is trapped, inhibiting sediment-bound nutrient transport to the stream. However, some studies have shown these VBS systems can promote subsurface nutrient loading to streams.

A study by Polyakov et al. (2005) examined current research regarding riparian buffer systems and their ability to retain nutrients. Their findings suggested that conditions, such as the spatial variability in soil hydraulic conductivity, the presence of preferential flow pathways, and limited storage capacity in the riparian zone's soil, could subvert the buffer system's ability and allow for increased nutrient transport. Osborne and Kovacic (1993) showed VBS could actually act like a nutrient source, releasing dissolved and total P into the ground water throughout the year. Another study conducted in Sweden showed that the soil in riparian zones had almost no P retention capacity due to a natural calcium leaching process which started over 3000 years ago (Vanek, 1993). Also, a study by Cooper et al. (1995) showed a high P availability for ground water transport due to saturation of the riparian zone.

There have been several studies conducted in which observation wells were used to monitor the flow of nutrients in groundwater. Vanek (1993) noted groundwater P concentrations taken from 12 wells in a lake riparian zone ranged from 0.4 to 11.0 mg/L with an average of 2.6 mg/L. Carlyle and Hill (2001) monitored the behavior of P in the

subsurface in a river riparian zone. This study suggested that riparian areas can become saturated with P and lose their ability to retain it. They noticed higher soluble reactive phosphorus (SRP) concentrations (100 to 950 μg/L) in areas characterized by having soils with higher hydraulic conductivities buried under the top soils. The authors also developed relationships for SRP with dissolved oxygen and iron (Fe^{2+}).

Most research to date on nutrient transport has focused on surface transport. Owens and Shipatalo (2006) monitored surface runoff and subsurface P concentrations and found that the surface runoff concentrations were generally much higher than the subsurface. However, the findings mentioned above show that there is a potential for subsurface nutrient transport. Surface runoff usually consists of high flows over a short period of time, whereas subsurface flow is usually characterized by lower flow rates over long periods of time. The point here is that even though the surface runoff has shown higher concentrations, low-concentration subsurface flow occurring over a long period of time could still be making a viable contribution to the total nutrient load of a surface water body. Therefore, there is a need for more research devoted solely to monitoring and evaluating the subsurface transport of P.

2.2 Subsurface Fate and Transport Processes

There are many different fate processes which P can undergo after it enters the soil matrix, such as sorption, uptake, and mineralization (Figure 2.1). One process by which P can be removed from the system is by plant uptake. When plants uptake P from soil solution in the root zone, a concentration gradient is created. In response, a diffusion

process across the soil solution begins to occur and more P is removed until the plant has used all it needs or is harvested.

Next, P can be partitioned between organic and inorganic pools and within different water and soil phases. From Figure 2.1 we can see that P can be divided into many groups. Organic P consists of applied organic P fertilizer, P present in plant residue and P found in soil organic matter. Other sources of P come from atmospheric deposition and from application of mineral fertilizers. Organic and inorganic P is then available for processes such as adsorption and precipitation.

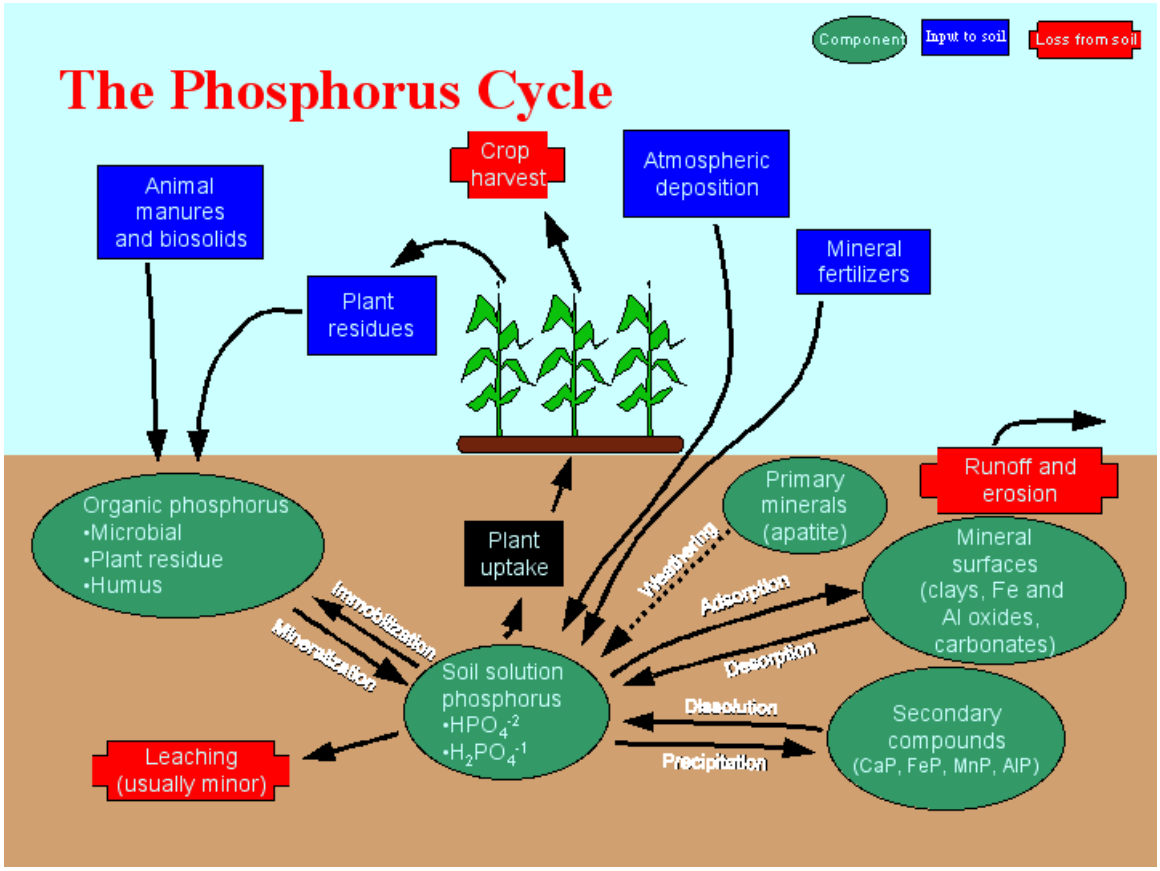

Figure 2.1. Various pools of P and their interactions with the soil matrix (http://msucares.com/crops/soils/images/phosphorus.gif).

Some of the P will go into solution form. The remaining P will either sorb to the surrounding mineral surfaces, usually forming Fe and Al oxides, or precipitate into secondary compounds. This sorption process can be either equilibrium or kinetic. The equilibrium group consists of the P which is strongly sorbed to the soil particles. The kinetic group refers to the P which may be weakly sorbed to the soil and is released into solution at some point after it initially enters the groundwater. This theory originated when researchers began noticing slight increases in P concentration over time when performing lab experiments. The only explanation for this comes from P that is initially sorbed being released from their "kinetic sorption" sites according to some reaction rate constant.

Carlyle and Hill (2001) highlight the release of P from stable and kinetic sorption sites into the solution pool due to changes in water chemistry within different zones of a riparian floodplain. They monitored how P dynamics changed due to hydrologic flow paths, lithology, and redox chemistry in a riparian floodplain. Their data showed higher concentrations of SRP were detected in buried river channel sediments underneath the topsoil compared to the soils located at the river margin. These buried channels consist of soils or gravels with higher hydraulic conductivities. The areas of high SRP also occurred with elevated levels of dissolved iron (Fe^{2+}) and reduced dissolved oxygen (DO) levels when compared to other sampling sites. They suggested that riparian areas might actually be contributing to the release of P because they increased the redox potential.

This can be explained using some principles of water chemistry. In order for low DO levels to exist, the water would have likely been present in the subsurface for a long time. This gives microorganisms more time to use the oxygen in the water for biological

processes and in turn depletes the DO. When DO is depleted, the redox potential of the soil increases. When the redox potential of the soil increases, metals like iron (Fe^{3+}) and aluminum (Al^{3+}) gain electrons and convert to Fe^{2+} and Al^{2+}. When this process occurs, phosphates (PO_4^{3-}) that were initially sorbed to the Fe^{3+} and Al^{3+} are released into solution. This is why higher SRP concentrations were observed in areas with low DO and high iron concentrations.

Another method of subsurface P transport is known as colloid-facilitated transport. Colloids are substances with tiny, non-diffusable particles that are suspended in a solution. They generally consist of soil particles less than 10 μm in diameter. The mechanism for this transport occurs when soluble P sorbs to the tiny soil particles in the colloid. The solution then moves through the pore spaces in the vadose zone. This is all determined by the size and stability of the colloids and the geometry of the soil particles (de Jonge et al., 2004). de Jonge et al. (2004) showed that spatial heterogeneity strongly affects actual colloid transport and leaching of strongly adsorbing P. Other studies noted significant amounts of particulate P when monitoring drainage from field catchments and tile-drained fields (Grant et al., 1996, Laubel et al., 1999.

2.3 Hydraulic Conditions Promoting Subsurface Phosphorus Transport

Local or regional conditions can lead to conditions where subsurface transport is important (Andersen and Kronvang, 2006). Areas such as riparian floodplains commonly consist of alluvial deposits possessing hydraulic properties conducive to the subsurface transport of P. These gravelly or cherty soils are common throughout the Ozark region of Oklahoma, Arkansas, and Missouri. In eastern Oklahoma, cherty soils adjacent to rivers

in the Lake Eucha/Spavinaw basin consist of gravelly silt loam to gravelly loam substrate below a thin layer of organic matter (Figure 2.2). The cherty soils include the following soils series of excessively drained soils formed in hill slope sediments: Clarksville (loamy-skeletal, siliceous, semiactive, mesic Typic Paleudults), Nixa (loamy-skeletal, siliceous, active, mesic glossic fragiudults), Coulstone (loamy-skeletal, siliceous, semiactive, mesic Typic Paleudults), Noark (clayey-skeletal, mixed, semiactive, mesic Typic Paleudults), and Wilderness (loamy-skeletal, siliceous, active, mesic Oxyaquic Fragiudalfs). A map of their distribution in the Lake Eucha/Spavinaw basin indicates that three of these soil series (Clarksville, Nixa and Noark) are prevalent features of the landscape (Figure 2.2).

An example of a typical pedon is shown in Table 2.1. The Clarksville series dominates the soil types in the lower portion of the watershed. Particle size averages 18 to 35% clay, 5 to 40% sand, and 35 to 70% rock fragments. Sauer and Logsdon (2002) studied the hydraulic properties of some of these cherty soils (Clarksville and Nixa) and concluded that relatively subtle morphological factors can have a disproportionate impact on water flow in the soils, suggesting the need for further research regarding their hydraulic properties. These soils possess infiltration rates as ranging from 1.22 to 3.67 m/d according to USDA Soil Surveys. Therefore, the potential for subsurface transport is significant. Research by McCarty and Angier (2001) focused on studying preferential flow pathways that existed in riparian floodplains. Their findings showed increased biological activity in these pathways and suggested a decrease in the ability to store nutrients. Current best management practices aimed at reducing P load through surface

runoff may be ineffective if subsurface flow is a significant transport mechanism and therefore could impact long-term planning of available water supplies in Oklahoma.

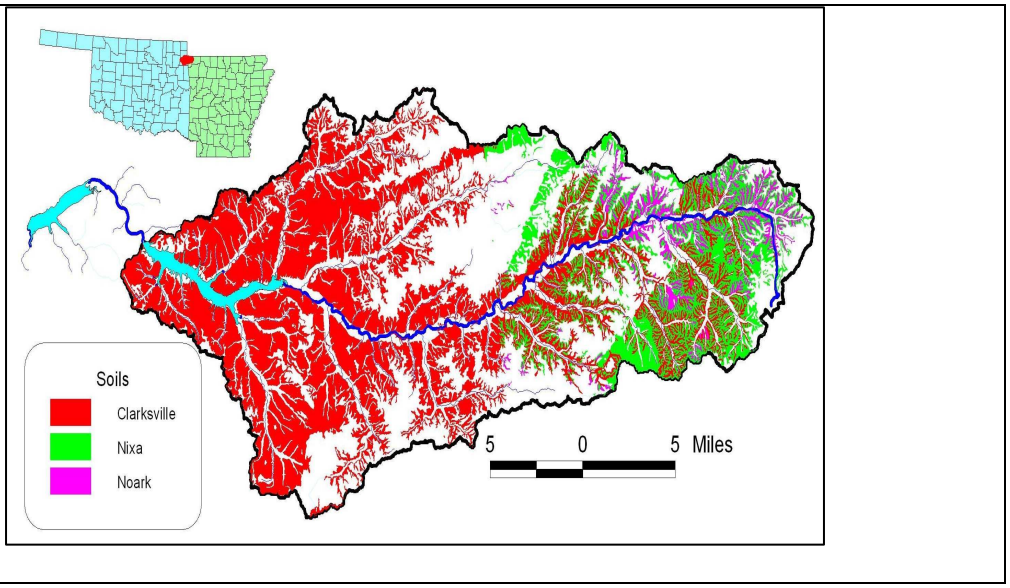

Figure 2.2. Map of the distribution of cherty soils within the Eucha/Spavinaw basin.

Table 2.1 Typical pedon for Clarksville cherty soils common in Ozark region of Oklahoma and Arkansas.

Horizon	Depth Increment (cm)	Soil Type/Description
0i	0-2	Decomposed Organic Matter
A	2-12	Dark Grayish Brown (10YR 4/2) Gravelly Silt Loam
E	12-30	60% Light Yellowish Brown (10YR 6/4) and 40% Brown (10YR 5/3) Gravelly Silt Loam
Bt1	30-46	Light Yellowish Brown (10YR 6/4) Gravelly Silt Loam
Bt2	46-74	Yellowish Brown (10YR 5/6) Very Gravelly Loam
2Bt3	74-104	Yellowish Brown (10YR 5/6) Extremely Gravelly Clay Loam
2Bt4	104-132	Strong Brown (7.5YR 5/6) Very Gravelly Clay Loam
3Bt5	132-152	Red (2.5YR 4/6) Cobbly Clay

Although there is an understanding of the P cycle, there is a lack of research and knowledge on the overall magnitude of P transport in the subsurface. Previous research has suggested that areas designed to retain nutrients can become saturated with P. The question is whether the potential sorption of P from the infiltrated water limits transport to streams. If it is saturated, then the question becomes what the desorption and/or precipitation potential from these subsurface soils is. It is hypothesized that the subsurface P load could potentially be significant at sites with these cherty soils because of the material's transport capability. The high conductivity of the cherty soils means less contact time between solution and solid phases and most likely, less sorption. The eventual scientific impact will be to determine if subsurface P transport is important on these landscapes and if so, what impact, if any, are current management practices having on this P source.

CHAPTER III

METHODOLOGY

In order to study the potential for subsurface transport in a riparian floodplain, a trench-piezometer system was installed in a riparian floodplain adjacent to the Barren Fork Creek near Tahlequah, OK (Figure 3.1). The trench system was designed to induce a constant water head and a tracer/P injection source on the subsurface alluvial gravel with subsequent monitoring of flow, tracer, and P transport in the piezometer field.

Figure 3.1. Field site located approximately 25 km east of Tahlequah, Oklahoma adjacent to the Barren Fork Creek.

3.1 Trench Location

The proposed site for the trench was located where the cherty, gravel layer was bounded by a relatively impermeable bedrock layer in order to induce water flow laterally through the soil profile above it. In order to determine the soil profile beneath the surface, two methods were used. First, ground penetrating radar (GPR) readings were taken every 25 cm along a 100 m transect. The data output showed differences in the soil profile that might represent where the gravel channels were present, but indicated no impermeable bedrock.

Next, sample trenches were dug along the same transect as the GPR readings to determine the accuracy of the GPR. Based on the profiles observed in the sample trenches, it was determined that the gravel layer occurred between 120 cm and 150 cm below the ground surface at all sampling locations. Disturbed gravel layer samples suggested that the alluvial gravel was homogeneous and initiated at a fairly uniform depth throughout the site. The thickness of the gravel layer could not be determined due to limitations on the dig depth of the excavator, which was between 3 and 4 m. No bedrock layer was encountered at any of the sampling locations along the 100 m transect. Because there was no optimum location in which the gravel layer was known to be bounded by an impermeable layer, the site of the trench became relatively arbitrary. Therefore, a location for the trench approximately 20 m from the stream bank was chosen (Figure 3.2).

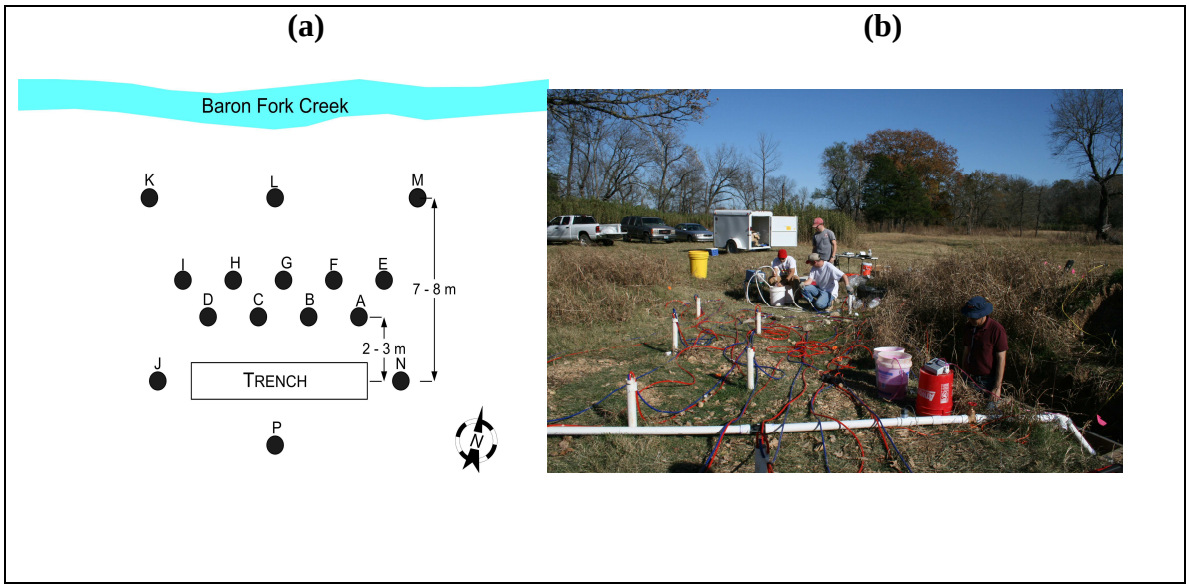

Figure 3.2. (a) Location of the trench and piezometers and (b) illustration of piezometers relative to the location of the trench. Photograph was taken from piezometer D looking northeast towards piezometers A and E.

3.2 Trench Installation

The trench was installed using a backhoe. The dimensions of the trench were approximately 0.5 m wide by 2.5 m long by 1.2 m deep. The bottom of the trench was located approximately 25 to 50 cm below the interface between the topsoil and gravel layers. In order to prevent the trench walls from collapsing, it was necessary to build a support system. This bracing system consisted of a frame constructed with 5 cm by 13 cm studs and covered with 2 cm plywood. The top and bottom were left open (Figure 3.3). Along with bracing the walls of the trench, this design allowed the water to infiltrate directly into the gravel layer.

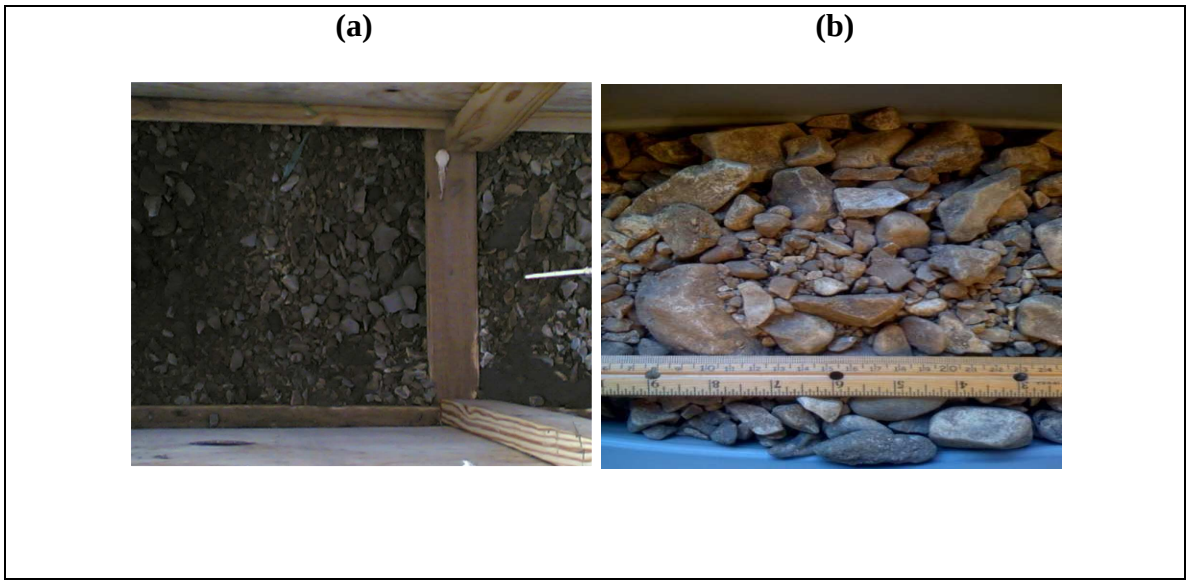

Figure 3.3. (a) Illustration of the bottom of the trench located just below the gravel/topsoil interface and (b) photograph of gravel sample to illustrate particle size.

3.3 Piezometer Installation

Fifteen piezometers were installed at various locations around the trench with the majority of the piezometers located between the trench and the river (Figure 3.2). The piezometers were approximately 6 m long and were constructed of 5 cm diameter Schedule 40 PVC. Each consisted of either a 3 m or 6 m screened section at the base. The piezometers were installed using a Geoprobe drilling machine, which used a hydraulic press and hammer to push a steel tube (7.6 cm diameter, 120 cm long) into the soil. Once a tube was driven to about 10 cm above ground surface, another tube was threaded onto it. This was continued until a desired depth was reached. For our case, once a depth of 6 m was reached, the 5-cm diameter piezometers were lowered down the 7.6-cm drill shaft and used to dislodge an expendable tip on the end of the steel tube. Next, the steel tube was pulled up, leaving the piezometer in place.

3.4 Soil Sampling

Core samples for the topsoil were taken at varying distances (3.0, 6.0, and 12.0 m) from the trench using a Giddings hydraulic drilling machine. The samples were obtained by pushing a 5-cm diameter, 120-cm long steel tube with a plastic liner to the desired depth. The tube was then retracted and the plastic liner containing the soil profile was removed. The topsoil samples generally consisted of soil from just below the surface to depths of about 1.5 m. It should be noted that core samples could not be obtained for the gravel layer. It was too difficult for the Giddings machine to push through this layer without damaging the equipment. Therefore, samples from the gravel profile were taken when digging the trench with the backhoe. Once the gravel layer was reached with the backhoe bucket, the trench walls began caving in when trying to dig deeper. Therefore, only the top of the gravel layer could be sampled. Although these samples were disturbed, they still provided a representation of the subsoil.

The samples taken from the gravel layer were analyzed for soil properties. The samples were first sieved to determine the particle size distribution for the gravel subsoil. After oven drying the sample, the coarse gravel was first separated out using a stack of five sieves ranging from 25.4 mm to 4.75 mm (No. 4). Next, the smaller particles were sieved using a sieve stack as follows: 4.75 mm (No. 4), 2.0 mm (No. 10), 0.85 mm (No. 20), 0.6 mm (No. 30), 0.425 mm (No. 40), 0.25 mm (No. 60), 0.15 mm (No. 100), and 0 mm (pan). Each sample was shaken for approximately 10 to 15 minutes on a vibratory sieve shaker. After shaking, each sieve was weighed to determine the mass retained for each particle diameter. This produced a distribution of particles by mass.

The particle size distribution was analyzed to determine the D_{10}, D_{30}, D_{50}, and D_{60} (i.e., diameter of soil particle in which 10, 30, 50, and 60%, respectively, of the sample is finer). Two properties determined from the particle size analysis were the uniformity coefficient, C_u and the coefficient of curvature, C_c, using equations (1) and (2):

$$C_u = \frac{D_{60}}{D_{10}} \tag{1}$$

$$C_c = \frac{D_{30}^2}{D_{60} D_{10}} \tag{2}$$

The uniformity coefficient is a parameter which indicates the range of distribution of grain sizes in a soil sample. A large C_u suggests a well graded soil, where a number closer to one means that all of the soil particles are approximately equal size. Das (2002) suggests that for a gravel to be considered well-graded, C_u should be greater than 4 and C_c should be between 1 and 3.

Once the particle size was known, the diameters were used with an empirical equation proposed by Alyamani and Sen (1993) to estimate the hydraulic conductivity of the gravel subsoil:

$$K = 1300\left[I_0 + 0.025\left(D_{50} - D_{10}\right)\right]^2 \tag{3}$$

where K is the hydraulic conductivity in m/d, D_{50} and D_{10} are the particle diameters in mm at which 50 and 10% of the sample is finer, respectively, and I_0 is the intercept of the line formed by D_{50} and D_{10} with the grain size axis (x-axis). This estimate for hydraulic conductivity was compared to another estimate obtained using a falling head test (Landon et al., 2001). The falling head test was performed by pumping water out of the Barren Fork Creek and into the trench until steady state conditions were reached. The pumps were then shut off and water levels were recorded over time as the trench drained. A

meter stick was attached to the side of the trench to allow for accurate readings while the water level in the trench decreased. The numbers obtained from the falling head experiment were then used with the Darcy and Hvorslev equations to estimate the vertical hydraulic conductivity:

$$K_v = \frac{L}{t_1 - t_0} \ln \frac{H_0}{H_1} \tag{4}$$

$$K_v = \frac{\frac{\pi}{11}\frac{D}{m} + L}{t_1 - t_0} \ln \frac{H_0}{H_1} \tag{5}$$

where K_v is the vertical hydraulic conductivity of the soil in m/d, L is the sediment interval being tested in m (0.25 to 0.5 m), H_0 and H_1 are the displacement in m of the water at time t_0 and t_1 respectively, D is the diameter of the device and m is the isotropic transformation ratio (assumed to be unity).

After sieving the soil sample, particles with a diameter less than 2.0 mm (No. 10 sieve) were further analyzed for P sorption capabilities. Phosphorus adsorption isotherms were estimated by adding different levels of P (0, 1, 5, 10, 25, 50, 100, 200, 400, and 800 mg P/L) to 2.0 g soil samples. The samples were shaken for 24 hours using a reciprocating shaker and then centrifuged for 10 minutes at 10,000 rpm. The P in solution was then quantified using ICP-AES analysis. Data were fit to linear and Langmuir isotherms to provide information in regard to the ability of the fine sediment fraction of the alluvial soils to adsorb P from solution:

$$q_e = K_d C_e \tag{6}$$

$$q_e = Q^O \frac{bC_e}{1 + bC_e} \tag{7}$$

where q_e is the mass of P sorbed per unit mass of soil, C_e is the equilibrium, dissolved phase P concentration, K_d is the distribution coefficient, and Q^0 and b are parameters of the Langmuir isotherm (i.e. Q^0 is the mass of P sorbed per unit mass of soil at complete surface coverage and b is the binding energy).

An ammonium oxalate extraction was also performed on the fine material to determine the degree of P saturation, which is the ratio of P to the total amount of iron and aluminum (Iyengar et. al 1981, McKeague and Day 1966, and Pote et. al. 1996). This procedure dissolved the non-crystalline forms of aluminum and iron in the material, considered to be the main sink for P among acidic soils. Therefore, selective dissolution of these amorphous minerals liberated any P associated with them into solution.

3.5 Tracer and Phosphorus Injection Experiments

Two Rhodamine WT tracer and one P (KH_2PO_4) injection experiments were performed to monitor subsurface movement from the trench (Table 3.1). Prior to the injection, each piezometer was sampled and analyzed for background P levels. Also, a water level indicator was used to determine the depth to the water table in each piezometer prior to injection. This would give a representation of the hydraulic gradient in the subsurface. Next, water was pumped from the Barren Fork Creek into the trench at approximately 0.0044 m^3/s in order to induce water movement. The water level in the trench was held as constant as possible at approximately 40 to 60 cm above the bottom of the trench for experiments 1 and 2, respectively. Water levels in the piezometers surrounding the trench were monitored over time. Prior to the KH_2PO_4 injection

experiment, background concentrations of P were monitored in the piezometers and in the Barren Fork Creek.

Table 3.1. Summary of Rhodamine WT and phosphorus (KH_2PO_4) injection experiments.

Experiment No.	1	2	3
Injection Compound	Rhodamine WT	Rhodamine WT	KH_2PO4
Concentration (ppm)	100	3	100
Compound Injection Duration (min)	60	90	90
Duration of Water Injection (min)	120	200	200
Average Water Level in Trench (cm)	44	60	60

Pumping continued until the system reached pseudo-steady state conditions, which was verified when the water levels in the piezometers remained constant. Once the system had reached steady state, either Rhodamine WT or P (KH_2PO_4) was injected into the trench at a constant rate using a variable rate chemical pump (Table 3.1). The solutions for Rhodamine WT and KH_2PO_4 were injected at a constant rate for either 90 or 120 min.

Once the injection began, samples were taken from the piezometers for the duration of the experiment in order to monitor the movement of the Rhodamine WT tracer and KH_2PO_4. To sample the piezometers, a peristaltic pump was used. In order to obtain water samples at two different depths for experiment 2 and 3, two hoses were run to each of the piezometers. One hose was lowered to a depth 10 cm below the water table, while another was lowered to a depth 110 cm below the water table. Each of the two hoses from the piezometers was run to a central location where they could more

easily be connected to the peristaltic pump. This was the most time-efficient setup when considering the number of piezometers that needed to be sampled.

The samples were placed into small bottles, put into a refrigerated cooler, and transported back to the lab where they were analyzed for Rhodamine WT, P and other cations such as calcium and aluminum. Each sample was analyzed for Rhodamine WT content using a Turner model 111 fluorometer and an Aquaflor handheld fluorometer. Samples were then analyzed for P content using two different methods. The Murphy-Riley (1962) method was used to measure the dissolved inorganic P present in the samples, while an inductively coupled plasma atomic emission spectroscopy (ICP-AES) machine was used to measure the total P present in the solution.

3.6 Laboratory Column Experiments

The fine material (i.e. diameter less than 2.0 mm) obtained from the sieve analysis was also used in a laboratory flow-through experiment to investigate the P sorption characteristics with respect to the flow velocity (DeSutter et. al. 2006). Approximately 5.0 g of the fine material was placed in each of six flow-through cells. This corresponded to a soil depth of approximately 2.3 mm. A Whatman 42 filter was placed at the bottom of each cell to prevent the fine material from passing through the bottom. Each cell had a nozzle at the bottom with a hose running from the nozzle to a peristaltic pump (Figure 3.4). The pump pulled water with a predetermined P concentration through the cells and fine material at a known flow rate (mL/min). Two different speeds on the peristaltic pump were used to evaluate the effect that flow velocity had on P sorption. The flow

rates used averaged 0.4 mL/min for the low flow experiment and 14 mL/min for the high flow experiment. These flow rates corresponded to average flow velocities of 1.3 and 46 m/d, respectively. First, 20 mL of deionized water was pulled through the soil to determine the background P that was removed from the soil. Then, a KH_2PO_4 was injected into each cell at 1.0 ppm and kept at a constant head using a Mariott bottle system (Figure 3.4). The low flow experiment was run for approximately 8 hours, while the high flow experiment was run for 1 hour. This was done to achieve approximately equal P loads to each system. Samples were taken periodically throughout each experiment. The samples were analyzed in the laboratory for P and Ca using both the Murphy-Riley (1962) method and ICP-AES analysis.

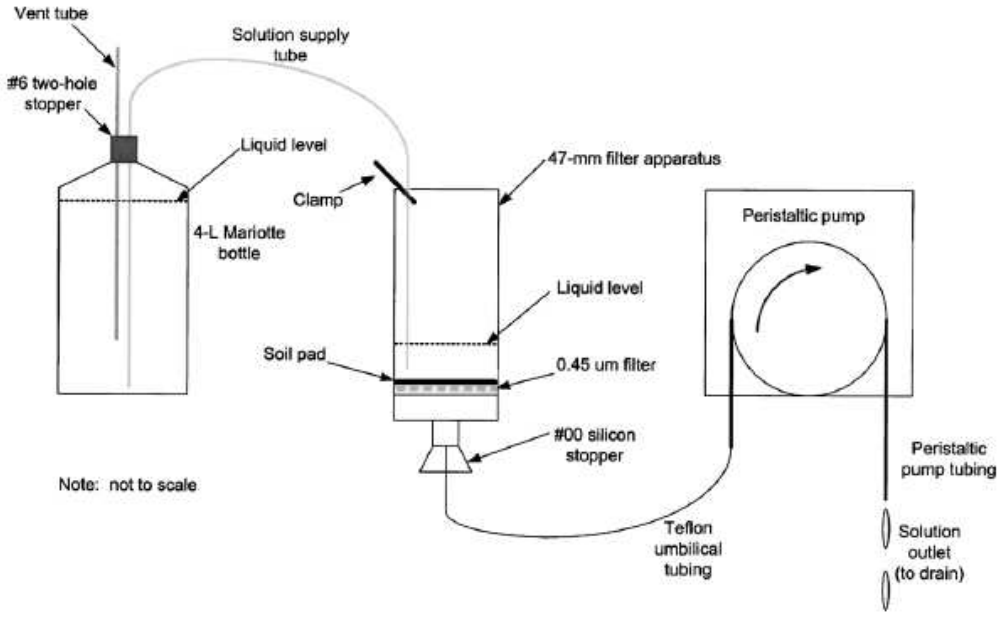

Figure 3.4. Laboratory flow-through experimental setup. (DeSutter et al. 2006).

The solution P concentrations obtained from the ICP-AES analysis were then used to evaluate the effect flow velocity on P sorption. Two scientific perspectives were used to analyze these data. The first method was based on contaminant transport theory

and compared the outflow P concentrations from both low flow and high flow velocities over time. The P concentrations determined by ICP-AES analysis were plotted versus a dimensionless injection time, t^*:

$$t^* = tQ/V_{ps},$$

where Q is the inflow rate and V_{ps} is the pore volume. The time was non-dimensionalized by multiplying the time at which the sample was taken by flow rate for each experiment and dividing by the pore volume. From the curve produced from outflow P concentration versus t^*, a breakthrough time, t_b^*, was estimated for each of the experiments. This was assumed to be the time at which 50% of the inflow concentration was detected in the outflow solution.

A sorbing contaminant moves through porous media at a retarded flow velocity, as suggested by the following advection-dispersion-retardation equations:

$$\begin{aligned} R\frac{\partial c}{\partial t} &= -v\frac{\partial c}{\partial x} + D_L^{(h)}\frac{\partial^2 c}{\partial x^2} \\ \frac{\partial c}{\partial t} &= -\frac{v}{R}\frac{\partial c}{\partial x} + \alpha_L\frac{v}{R}\frac{\partial^2 c}{\partial x^2} \\ \frac{\partial c}{\partial t} &= -v_s\frac{\partial c}{\partial x} + \alpha_L v_s\frac{\partial^2 c}{\partial x^2} \end{aligned} \qquad (8)$$

where x is the direction along the length of the column, c is the concentration, v is the pore water velocity, $D_L^{(h)}$ is the hydrodynamic dispersion coefficient, α_L is the dispersivity, and v_s is the sorbed contaminant velocity. The sorbed contaminant velocity is simply the groundwater velocity divided by the retardation factor, R, and describes the reduced rate at which a sorbing contaminant moves through the soil. Solutions to these one-dimensional equations were given by Ogata and Banks (1961) and Hunt (1978):

$$C(x,t) = \frac{C_0}{2} erfc\left(\frac{x - v_s t}{2\sqrt{\alpha_L v_s t}} \right) \quad (9)$$

The data from the flow-through experiments were then used with this equation to inversely estimate v_s and α_L by minimizing the sum of squared errors between predicted and observed outflow concentrations (i.e., x = 0.23 cm). With this estimate for v_s, the average flow velocity measured during the experiment (v) was used to estimate R and then K_d. The K_d estimated from low-flow and high-flow velocity experiments was then compared with the K_d from the batch sorption tests.

Based on the one-dimensional advection-dispersion equations, a ratio relating the breakthrough times and flow velocities was derived assuming the length of the columns were equivalent between flow velocity experiments:

$$\frac{v_h}{v_l} = \frac{t_{b_l}}{t_{b_h}} \quad (10)$$

where t_{b_l} and t_{b_h} are the breakthrough times and v_h and v_l are the velocities for the high flow and low flow tests, respectively. The derived equation suggested that the ratio of the flow velocities for the high flow and low flow tests were proportional to the inverse of the breakthrough times for each velocity. If these ratios were approximately equal, then equivalent transport processes (i.e., advection, dispersion, and sorption) were occurring for both flow velocities. If the ratios differed, then variable P sorption was occurring and the flow velocity had an effect on the sorption characteristics of the fine (i.e., less than 0.2 mm) material.

These data were also analyzed based on the concentrations of P in the outflow as measured by the ICP compared to the total amount of P added to the system. The

principle of this method was that if an equal mass of P was added to each system, the measured P concentrations in the outflows would be approximately equal if flow velocity did not have an effect on sorption. The mass of P added per kilogram of soil (mg P/kg soil) was found by multiplying *Q* (mL/min) by the inflow P concentration (mg/L) and by the elapsed time of the experiment (min). These data were plotted against the P concentrations (mg/L) detected in the outflow solutions for both flow velocities. In theory, if equivalent sorption was occurring, the curves associated with each data set would be approximately equal. If velocity had an effect on sorption, the curve for the low velocity data set would be lower than the curve for the high velocity data set.

CHAPTER IV

RESULTS AND DISCUSSION

4.1 Soil Properties

From the particle size analysis of the gravel subsoil, it was found that roughly 81% of the material by mass was larger than 2.0 mm (Figure 4.1). This was significant because 2.0 mm is generally considered the upper limit used when attempting to characterize the sorption properties of a material. In other words, 81% of the gravel subsoil would likely be considered to have negligible sorption capabilities. The other pertinent particle diameters used in calculating the uniformity coefficient, C_u, and the coefficient of gradation, C_c can be found in the legend included in Figure 4.1. For our sample, C_u was 22 and C_c was 2.3. These numbers suggest that the gravel subsoil was fairly well-graded.

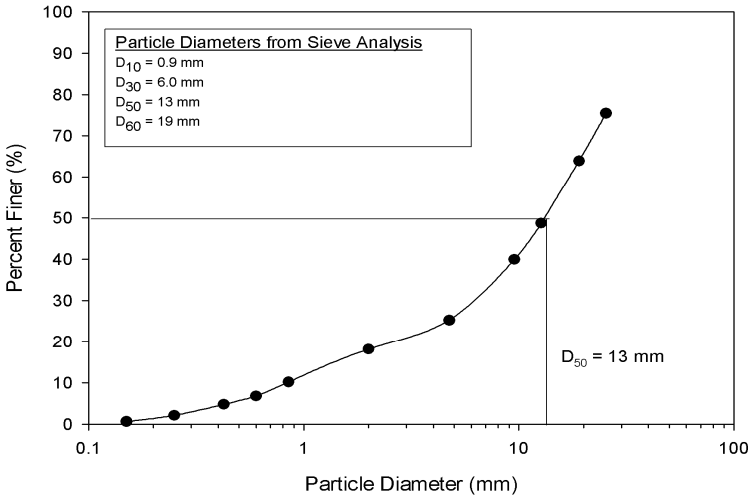

Figure 4.1 Particle size distribution for gravel subsoil in the riparian floodplain.

The particle size distribution was also used to estimate the hydraulic conductivity, *K*, of the gravel subsoil. Using a D_{50} of 13 mm, a D_{10} of 0.85 mm and I_0 equal to 0.4 mm, the hydraulic conductivity was estimated to be 640 m/d. Estimates for hydraulic conductivity, *K*, obtained from the falling head test data ranged from 150 to 220 m/d (Table 4.1). The estimates were much higher than the USDA NRCS soil survey estimates for the three main topsoils in Cherokee County (Table 4.1). This could be due to the fact that most of the equations used to calculate *K* previously focused on soils with much smaller grain sizes (Landon et al., 2001). As indicated in the particle size distribution, the alluvial system tested here had a large percentage of gravels greater than 10 mm in diameter. Although the estimates for hydraulic conductivity obtained from the particle size distribution and falling head test may be elevated representations of the *K*, they still demonstrated how conductive the gravel subsoil was and could be used as an indicator of the potential for rapid water and nutrient transport in the alluvial system.

Table 4.1. Hydraulic conductivity estimates from tests conducted on disturbed soil samples for the gravel subsoil versus USDA-NRCS soil surveys for topsoils.

Baron Fork Field Sample		USDA Soil Survey, Cherokee Co., OK	
Equation Used	Hydraulic Conductivity, K (m/d)	Soil Type	Hydraulic Conductivity, K_s (m/d)
Alyamani & Sen	640	Clarksville	2.5
Darcy	150	Elsah	6.7
Hvorslev	220	Britwater	0.8

The fraction of alluvial deposit less than 2.0 mm (i.e. about 19%) was found to possess considerable sorption capability based on linear (K_d = 2.0 L/kg based on C_e = 50 mg/L) and Langmuir (Q^0 = 125 mg/kg and b = 0.048 L/kg) isotherms. However, when

compared to other Oklahoma soils analyzed for P sorption properties, the Q^0 determined for our sample (125 mg/kg) was lower than any other soils analyzed in Eastern Oklahoma (Table 4.2).

Table 4.2. Values for P sorption maximum, Q^0 and Binding Energy, b for Oklahoma topsoils (Fuhrman, 1998).

Soil Type	P sorption maximum, Q^0 (mg/kg)	Binding Energy, b (L/kg)
Sallisaw	772	4.32
Cahaba	703	2.57
Shermore	698	2.87
Carnisaw	599	1.19
Stigler	580	0.92
Captina	542	3.84
Rexor	506	1.29
Kullit	465	3.16
Ruston	343	1.41
Gallion	191	1.03

Results from the ammonium oxalate extractions showed a degree of P saturation of 4.2% when not including the alpha factor of 0.5 (Beauchemin and Simard 1999). This alpha factor has been used to adjust the total amount of iron and aluminum that could be available in different soil types. The value was derived from a given set of soils and laboratory conditions. Thus, it may not be appropriate for use in all cases. When incorporating the alpha factor of 0.5, the degree of P saturation for the fine soil was found to be 8.4%. Both P saturation values could be considered lower than agricultural topsoils with a history of P applications beyond crop needs. This suggested that the fine soil material was capable of sorbing a considerable amount of P. However, this only pertains to the fine material in the gravel subsoil, which is only about 19% of the entire size fraction.

A weighted linear K_d calculated based on the 2.0 mm size fraction resulted in a K_d of 4.5. This weighted K_d suggested a P sorption retardation factor, R of 18 to 24 based on soil bulk density estimates, ρ_b for the gravel material of 1.5 to 1.8 g/cm^3 and porosity, ε, equal to 0.35 to 0.4, where R is defined as:

$$R = 1 + \left(\frac{K_d \rho_b}{\varepsilon} \right) \tag{8}$$

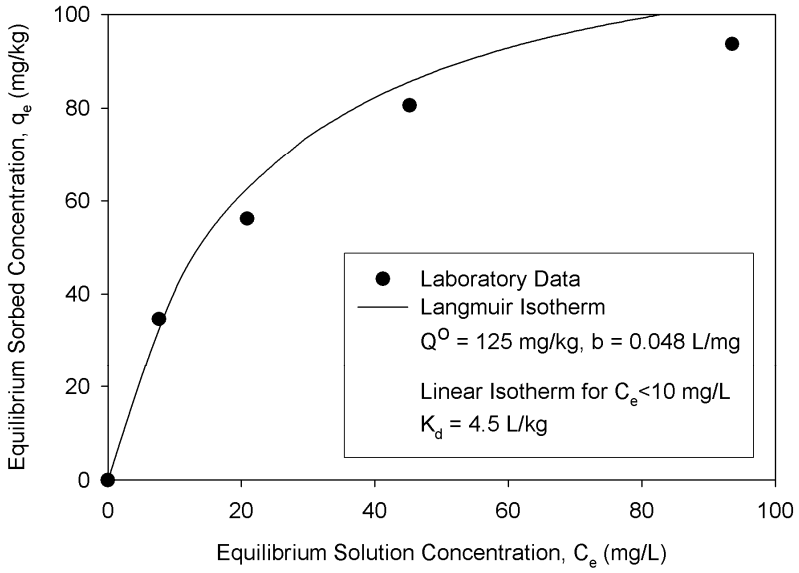

Figure 4.2. Laboratory data fit to Langmuir and linear isotherms to obtain sorption parameters for fine soil material (< 2.0 mm).

4.2 Tracer and Phosphorus Injection Experiments

In the first experiment, Rhodamine WT was injected at 100 ppm (Table 3.1). Samples analyzed from this experiment showed detectable concentrations in all of the piezometers. Concentrations detected in piezometers located 2 to 3 m from the trench (i.e. piezometers A, B, and C) peaked at 36 ppb with peak concentrations occurring

approximately 30 minutes after injection began. Detected levels in piezometers located 7 to 8 m from the trench (K, L, and M) were generally less than 30 ppb with peak concentrations occurring approximately 50 minutes after initiation of injection (Figure 4.3).

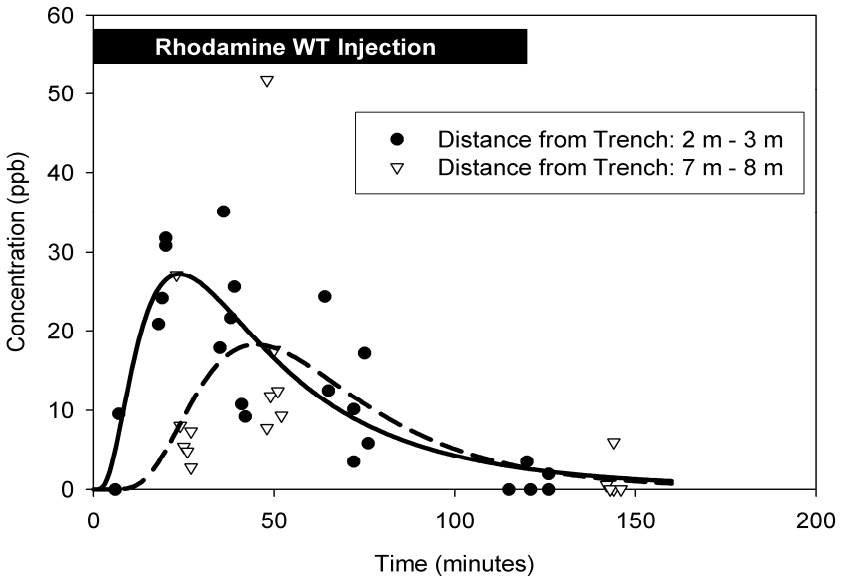

Figure 4.3. Rhodamine WT concentrations for piezometers located 2-3 m and 7-8 m from trench.

Also, Rhodamine WT concentrations detected in piezometers D, I, and J for the first experiment were much higher than those detected in all other piezometers (Figure 4.4). Sample concentrations from these piezometers all exceeded 300 ppb, which was the upper detection limit on the field fluorometer. After dilution in the lab, the concentrations in these piezometers were found to be close to the injected concentration of 100 ppm. Piezometers D, I, and J were hypothesized to be located in a preferential flow pathway which was more conductive than other subsurface material (Figure 4.4).

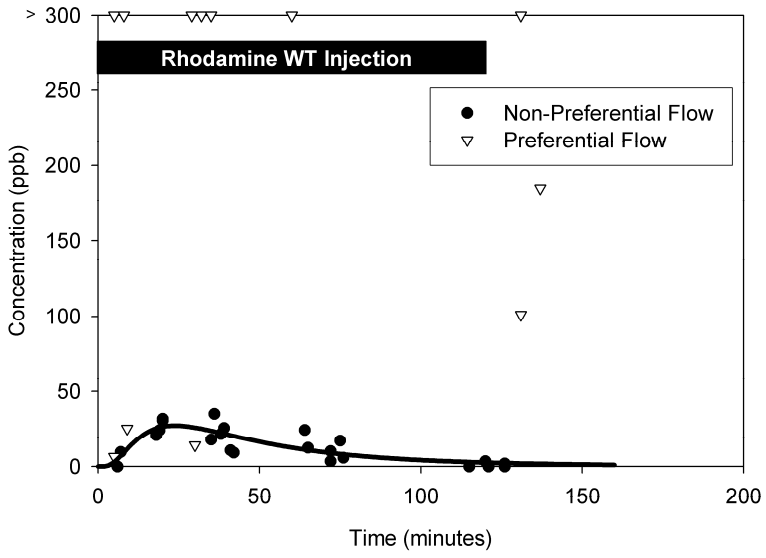

Figure 4.4. Rhodamine WT concentrations in preferential and non-preferential flow piezometers. Note: Concentrations > 300 ppb were above detection limit of field fluorometer.

In the second experiment, Rhodamine WT was injected at approximately 3.0 ppm with the intent of staying within the range of detection for the field fluorometer (Figure 4.5 (a). Sample analysis showed a pattern similar to the first injection, with detection levels in piezometers D, I, and J approximately equivalent to the injected concentration of 3.0 ppm (Figures 4.5). However, there was no Rhodamine WT detected in any of the other piezometers. This was hypothesized to be due to the fact that the injected concentration of 3.0 ppm (compared to 100 ppm in the first experiment) was diluted below detection limit by the time it reached the outer piezometers.

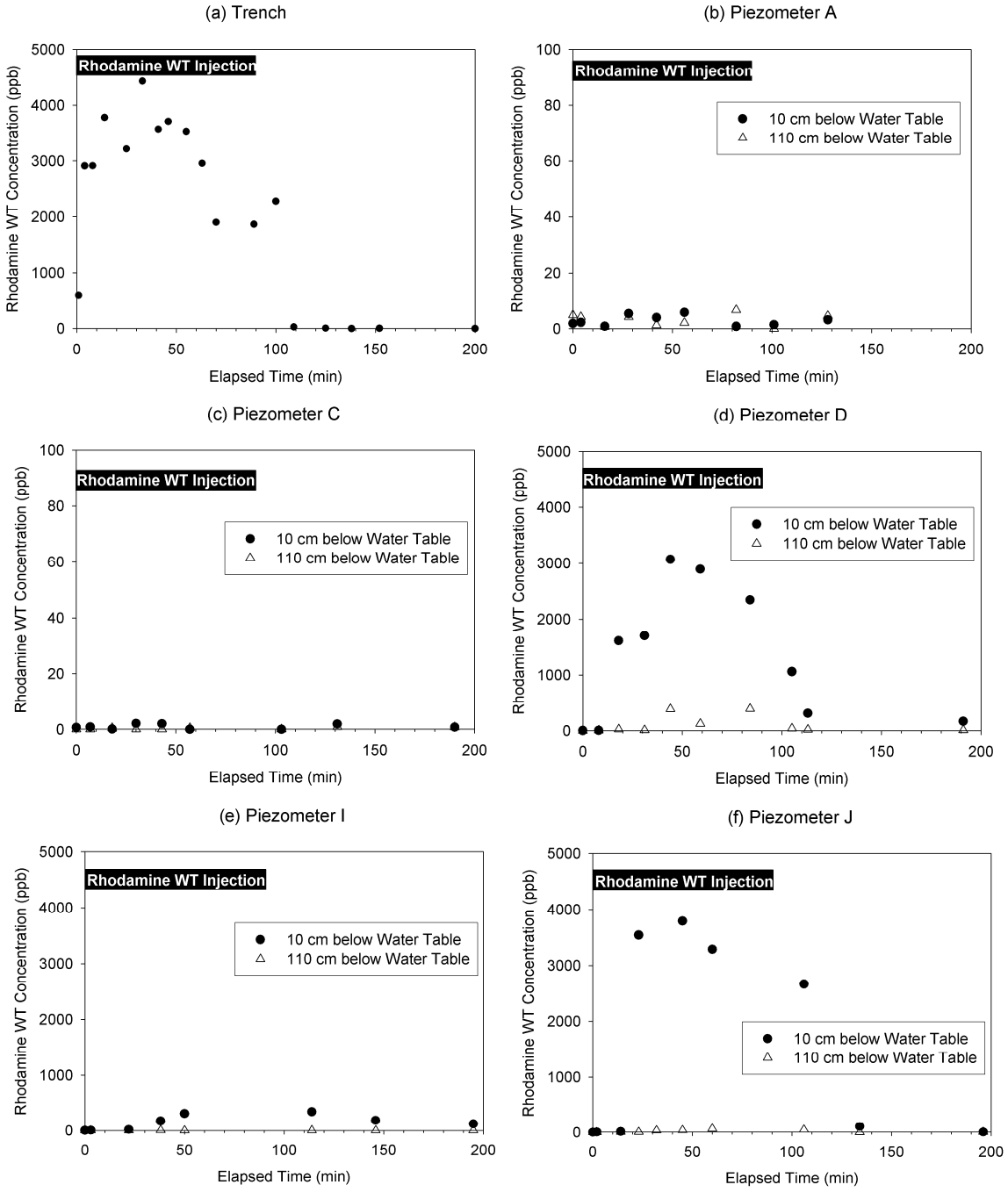

Figure 4.5. Experiment 2 - Rhodamine WT concentrations in trench (a) compared to non-preferential flow piezometers (b) and (c) and preferential flow piezometers (d), (e), and (f).

The results from the second Rhodamine WT injection supported the hypothesis that a highly conductive preferential flow pathway existed in the subsoil. The Rhodamine WT concentrations detected in the preferential flow pathway, i.e. figures 4.5 (d), (e), and (f) were roughly two orders of magnitude larger than the concentrations detected in the non-preferential flow piezometers, i.e. Figures 4.5 (b) and (c). This demonstrated the potential for rapid subsurface transport in this alluvial system. These preferential flow pathways in alluvial deposits could represent a direct connectivity with upland nonpoint source pollution sources.

Another trend visible from the Rhodamine WT injections was that samples taken from 10 cm below the water table showed significantly higher concentrations than samples taken 110 cm below the water table for the piezometers considered to be in the preferential flow pathway (Figure 4.5). These data supported the possibility of layering in the subsoil and suggested that the flow is large enough in the preferential flow pathways to inhibit vertical mixing.

Prior to the injection experiments, piezometers were sampled to determine the hydraulic gradient and background P levels. The water levels detected in each piezometer showed minor differences (i.e. less than 1 cm). Therefore, it was difficult to determine if a hydraulic gradient existed which was directed towards the preferential flow pathway. However, water level readings from 2 of the piezometers in the preferential flow pathway suggested that water was flowing down the side of the piezometer. Background P samples were grouped according to the observed piezometer flow response from the Rhodamine WT experiments: (1) preferential flow piezometers versus (2) non-preferential flow piezometers. A statistically significant difference ($\alpha = 0.05$) was

observed between the background P concentration in preferential versus non-preferential flow piezometers (Figure 4.6 and Table 4.3). Concentrations of P in the Barren Fork Creek were approximately 1.8 times higher than those observed in the piezometers. The difference between piezometer groupings suggested potential for the preferential flow piezometers to be more directly connected to the stream channel and non-point source loads in the stream.

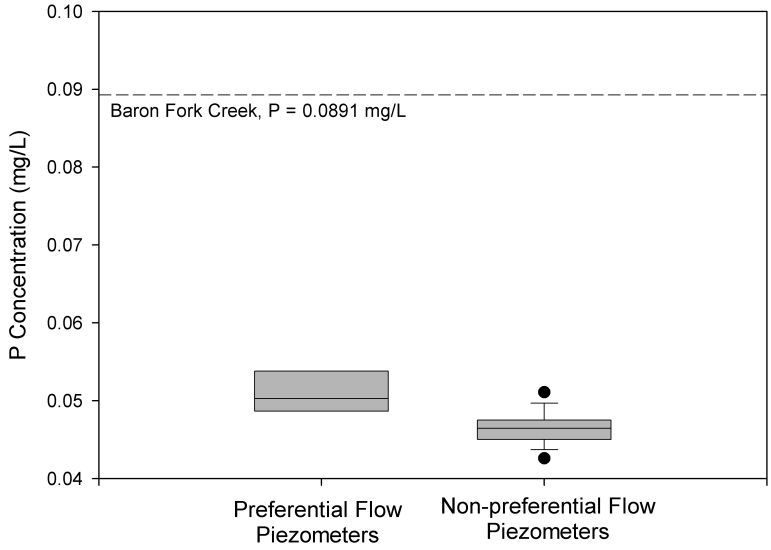

Figure 4.6. Experiment 3 - Box plots of background phosphorus (P) concentration in preferential flow versus non-preferential flow piezometers prior to P injection experiment. 25th and 75th percentiles = boundary of the box; median = line within the box; 10th and 90th percentiles = whiskers above and below the box.

Table 4.3. t-test two-sample assuming unequal variances on background P concentrations in preferential flow versus non-preferential flow piezometers for experiment 3.

	Preferential Flow Piezometers	Non-Preferential Flow Piezometers
Number of samples	6	24
Mean	0.051	0.047
Standard Deviation	0.003	0.002
t Stat	3.46	
P(T<=t) two-tail	0.013*	

* Statistically significant difference between the groups at $\alpha = 0.05$.

In the third experiment, KH_2PO_4 was injected into the trench at a concentration of 100 ppm, as shown in figure 4.7 (a). Similar to the Rhodamine WT injections, P concentrations in preferential flow piezometers again mimicked concentrations injected into the trench (Figures 4.7 (b) and (c). In non-preferential flow piezometers, P was not detected above background concentrations even in piezometers 2 to 3 m from the trench. These results suggested that sorption retarded the movement of P to these piezometers, and that no significant sorption was observed for piezometers D and J. Two hypotheses were proposed for the lack of sorption that was suggested in piezometers considered to be in the preferential flow pathway: (1) the presence of fewer particles with significant P sorption capability and/or (2) lack of contact time between aqueous and solid phases due to the higher flow velocities. To evaluate the first hypothesis, undisturbed soil cores were needed from the preferential flow path. However, these were difficult to obtain in the gravel substrate due to the large particle sizes encountered when trying to drive a

sampling core. Therefore, this hypothesis was not evaluated. The second hypothesis was evaluated using flow-cell experiments in the laboratory.

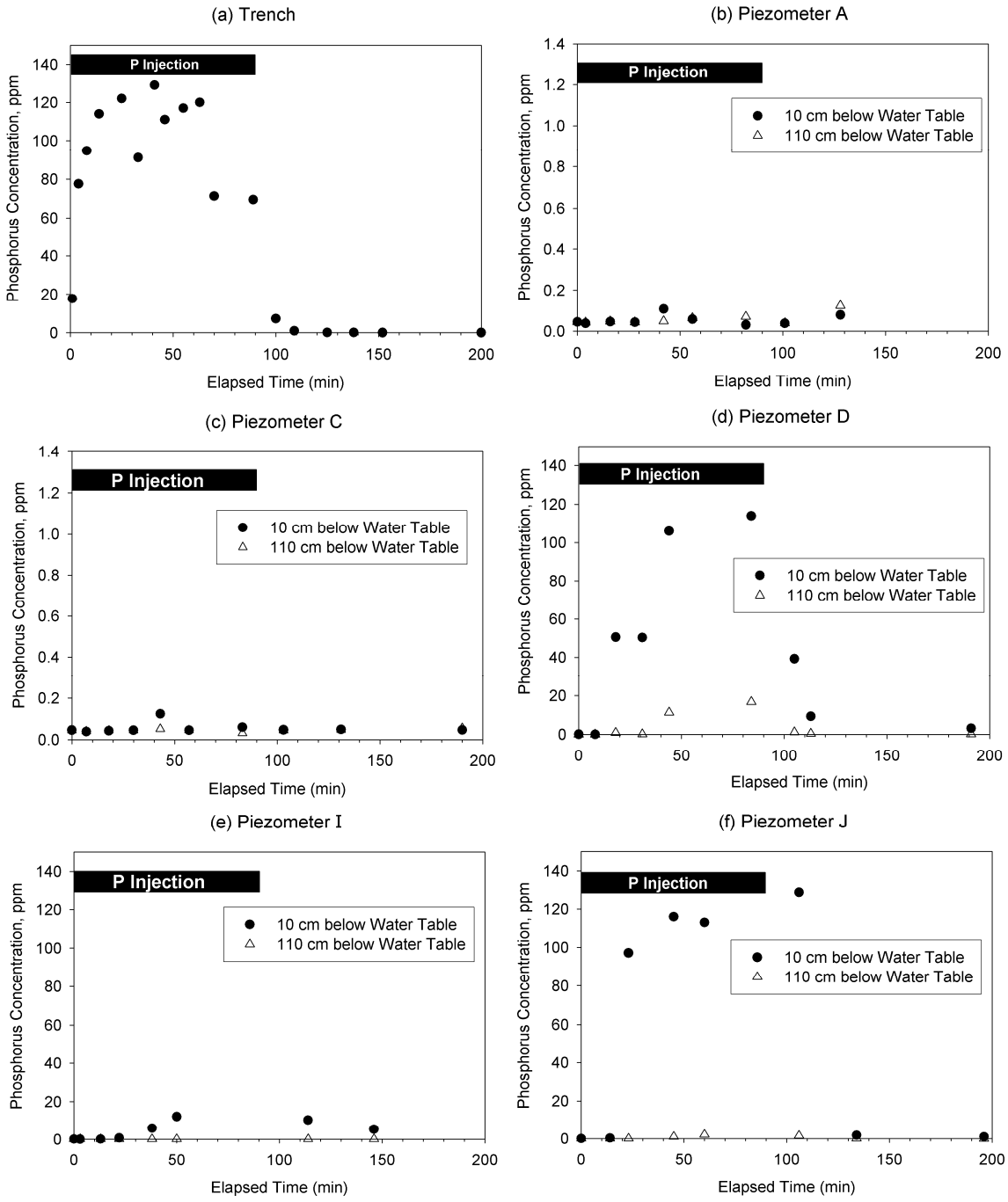

Figure 4.7. Experiment 3 - Phosphorus concentrations in trench (a) compared to non-preferential flow piezometers (b) and (c) and preferential flow piezometers (d), (e), and (f).

4.3 Laboratory Flow Experiments

Both the contaminant transport and load perspectives suggest that flow velocity had an effect on the sorption capabilities of the system. Figure 4.8 (a) shows the P concentrations for both velocities plotted versus dimensionless time. Concentrations detected in the outflow solution for the high velocity experiment are approximately 90% of the inflow P concentration after less than 1 min. Therefore, the breakthrough time, t_b, for the experiment is less than 1 min. The exact time at which 50% of the sample was detected is not known because the first sample (i.e., at 0.5 min) corresponded to 60% of the inflow concentration. The exponential fit to these data (Figure 4.8a) was used to estimate a t_b^* of 2.7, which corresponded to a t_b of 0.4 min. For the low flow experiment, the outflow concentration gradually increased with time and reached approximately 75% of the inflow concentration after 8 hrs of injection. The t_b determined for the low flow experiment was approximately 160 min, which corresponded to a t_b^* of 25 (Figure 4.8a).

These data suggested that greater P sorption to the soil was occurring in the low flow experiment. Specifically, the velocity ratio between the high-flow and low-flow experiments was approximately 36 when using average flow velocities of v_h = 46 and v_l = 1.3 m/d. Compared to the ratio of the breakthrough times of approximately 390, additional P sorption was occurring during the low-flow experiment. This could likely be due to the small reaction time between the P and soil surfaces during the high-flow experiment.

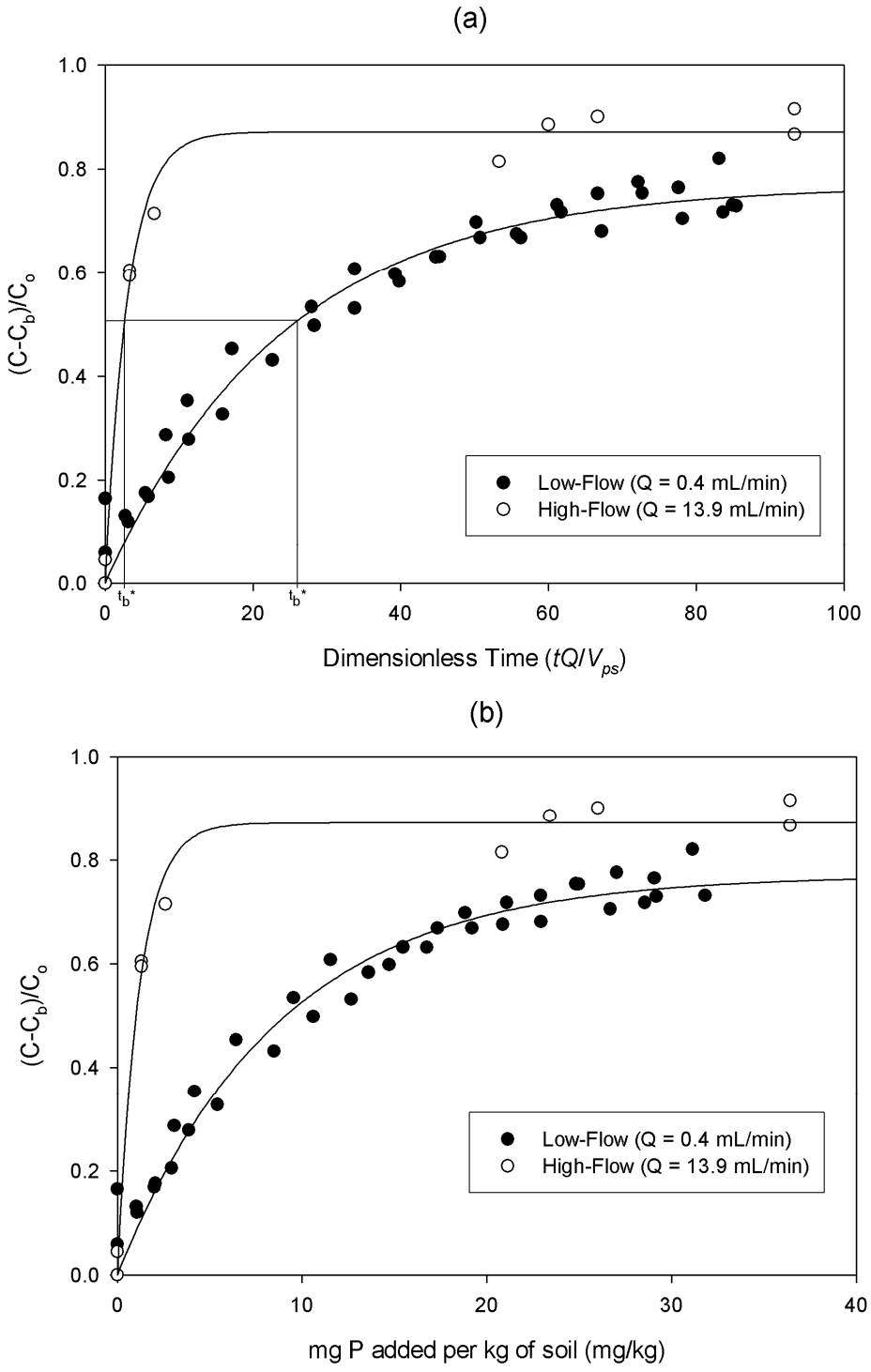

Figure 4.8. Phosphorus (P) concentrations detected in outflow (C) versus (a) dimensionless time and (b) mg P added per kg of soil, where Q is the flow rate, V_{ps} is the pore space volume, C_b is the background P concentration released from the soil, and C_o is the inflow P concentration.

The flow-through experiment data were also analyzed by comparing the P load added to the P concentrations detected in the outflow, as shown in Figure 4.12 (b). Variables such as inflow P concentration, mass of P added and mass of soil sample were held constant. The only parameter changed between the two experiments was flow velocity. From Figure 4.8 (b), it is noticeable that the outflow P concentrations detected for the low flow experiment were consistently less than the concentrations obtained during the high flow experiment at the same P load added. Similar to the contaminant transport analysis, these data also suggest that more P sorption was occurring during low flow velocity experiments and that flow velocity had an effect on sorption.

The results from flow cell experiments suggested that neither variation in fine particle distribution nor P sorption kinetics could be eliminated as factors hypothesized to contribute to the field-observed sorption in non-preferential pathways compared to preferential flow pathways. Most likely, a combination of both the presence of fewer fine particles (i.e. soil particles less than 2.0 mm in diameter which possess greater P sorption capability) and the lack of contact time between aqueous and solid phases due to the higher flow velocities in the preferential flow path contributed to the variability in P sorption observations. Estimates for K_d were obtained from the Ogata and Banks (1961) equation for both flow velocities (Table 4.4).

Table 4.4. Soil-water partition coefficients, K_d, estimated from batch sorption and laboratory flow experiments.

Experiment	K_d (L/kg)	SSE (%)
Batch	4.5	-
Low Flow	11	27
High Flow	0.9	1

The differences in the K_d values obtained from both the batch sorption isotherm test and the flow-through experiments suggested that nonequilibrium processes were occurring in the system. These processes can be divided into physical and chemical nonequilibrium. Physical non-equilibrium is the result of dissolved P moving into the micropores between the soil particles, resulting in an overestimation of P sorption. Because there was not a large amount of fine clay in the material, the effect of microporosity is likely negligible. Therefore, the differences in the K_d are likely due to a chemical kinetics, meaning that the amount of sorption observed varied due to the time associated with the reaction between dissolved P and the soil surfaces.

CHAPTER V

CONCLUSION

5.1 Summary and Conclusion

This research demonstrated that subsurface movement of P can be an important transport mechanism, especially in areas such as riparian floodplains with hydraulic conditions conducive to the rapid transport of P. The movement of water and contaminants in riparian floodplains is not homogeneous, and can be impacted by the presence of preferential flow pathways.

Using a trench-piezometer system, the subsurface transport of a conservative tracer (i.e., Rhodamine WT) and P solution was monitored while inducing flow in the system. Concentrations of both Rhodamine WT and P were equivalent at the injection point (i.e., trench) and at preferential flow piezometers located on the southwest side of the trench. However, concentrations of Rhodamine WT and P in non-preferential flow piezometers, some of which were within 2 to 3 m of the trench, did not mimic injected concentrations. Although Rhodamine WT was detected in non-preferential flow piezometers 2 to 3 m from the trench at concentrations near 40 ppb, P was not measured above background concentrations (i.e. 40 ppb) in these non-preferential flow piezometers.

The results suggested that P sorption may have occurred on the fine material along non-preferential flow pathways. Sorption of P to subsoil material in the preferential flow pathways was hypothesized to be minimal due to a combination of two factors: (1) the presence of fewer fine particles (i.e. soil particles less than 2.0 mm in diameter) and (2) lack of contact time between aqueous and solid phases due to the higher flow velocities. To test the second hypotheses, laboratory experiments were conducted. The flow-through experiments suggested that the velocity of flow through the subsoil had an effect on P sorption. When using the high flow velocity, the breakthrough time for P was estimated to be 0.4 min and concentrations reached 90% of the inflow concentration in less than 10 min. Using the low flow velocity, the breakthrough time for P was estimated to be 160 min and concentrations detected in the outflow increased at a much slower rate before peaking at approximately 75% of the inflow concentration after 370 min. The differences in the breakthrough times and outflow concentrations for each velocity suggested that sorption was occurring. This hypothesis was also supported when analyzing the flow through experiment data on a P load basis. When equal masses of P were added to each system and the only parameter altered was velocity, concentrations detected in the outflow solutions from the low velocity were consistently lower than those detected using the high velocity. If velocity had no effect on sorption, the values theoretically should have been the same.

These findings suggested that high concentrations of P (i.e., concentrations mimicking the injected concentration) detected in the piezometers located in the preferential flow pathway were a result of the greater flow velocity in this zone. The velocity, in turn, likely led to a smaller reaction time between the dissolved P and soil

surfaces, prohibiting measurable sorption. The lack of P detection in the non-preferential areas was also supported by the data from the low flow velocity experiment. These findings suggested that the lack of P detection in piezometers outside of the preferential flow pathway may have been a result of the P solution moving much slower through the subsoil and therefore sorbing to the fine material. This fine material consisted of secondary minerals with larger surface areas, such as kaolinite and non-crystalline Al and Fe oxyhydroxides, and is characterized by valence-unsatisfied edge hydroxyl groups. Due to the valency, these edge hydroxyl groups are highly active and account for the majority of P sorption in the material. Although isotherm data on the fine material showed that material had lower sorption properties than other surface soils in Oklahoma, it did suggest that the material was capable of sorbing P. Therefore, the finding that P was sorbing in the low flow experiment was reasonable.

This research has wide reaching implications for how riparian floodplains are managed. Millions of dollars are spent each year to mitigate surface runoff and sediment and nutrient loads. Although these management plans can be effective, this research has shown that subsurface P transport could also be a contributing factor in certain conditions. Because the nutrient load studied here was input directly into the subsurface, the overall subsurface contribution could not be quantified. The next step is determining if similar conditions like this are common and if a direct connection exists between nutrient sources on the surface and the conductive subsurface material.

This study demonstrated the heterogeneity that exists in the subsoil which can promote significant nutrient transport. Preferential flow pathways may create direct hydraulic connections between nonpoint source loads in the stream and the alluvial gravel

subsoil. These direct connections could lead to a transient storage mechanism, where upland nutrient loads concurrent with large storm events could potentially migrate downstream into the adjacent floodplain, contaminating the alluvial storage zone. Second, a direct connection may exist between upland sources of P and the streams such that a significant nonpoint source load may not be currently considered in analyzing for the impact of P application and management on such landscapes.

5.2 Recommendations for Further Research

This research showed that alluvial subsurface systems can have significant potential for nutrient transport. However, the study was only conducted over a short period of time. Previous research also showed that an alluvial system's hydrologic properties were highly spatially and temporally variable and this research supported that finding. It is unreasonable to think that the long term nutrient impact that subsurface systems have on surface water bodies could modeled simply based on this one study. Future work needs to focus on determining if similar processes are occurring in other riparian areas and finding common geological characteristics of these systems. This study also monitored an unnatural nutrient load input directly into the subsurface. Because of this, there is still a need for determining whether a direct connection exists between surface-applied nutrients and subsurface alluvial systems capable of rapid transport. As long as the overall nutrient contribution of subsurface alluvial systems compared to surface mechanisms is not known, research will continue to focus on mitigating nutrient inputs by reducing surface runoff.

Future research on similar riparian subsurface systems should also attempt to characterize the subsurface system in as much detail as possible in order to more accurately demonstrate the heterogeneities that occur within the subsurface. Electrical resistivity imaging could be used to map the subsurface profile and identify regions that could be conducive to rapid transport (i.e. preferential flow pathways). Once these areas were identified, they could be instrumented more accurately, sampled over much longer periods and analyzed in order to determine if processes similar to those found here were occurring in other areas.

Further work should also focus on transport both into and out of riparian areas. For example, once an area conducive to subsurface transport was identified, a conservative tracer could be injected into the stream itself and piezometers located along the stream could be sampled to determine if the tracer was moving into the riparian area as well as downstream. Future projects should also monitor over longer periods of time in hopes of more appropriately quantifying the magnitude of subsurface nutrient loading. Research could continue to use conservative tracers as a way of monitoring the transport potential but should also focus on monitoring the natural nutrient flow into and out of the subsurface areas and in the stream itself. This could help determine whether nonpoint source nutrient inputs upstream migrate into the riparian subsurface areas further downstream and whether or not these areas are actually sorbing nutrients or acting as a storage zone and transmitting them back into the stream during periods of low flow.

Results from these studies could then be used to focus on identifying geologic characteristics of the system that suggest that subsurface nutrient loading could be a problem. Ideally, these characteristics could then be expanded to a watershed scale in

hopes of isolating these areas. Once the areas sensitive to subsurface nutrient transport were identified, the work could shift to designing alluvial floodplain management practices which incorporated subsurface transport as a nutrient source. These alternative management practices could then be put in place in hopes of reducing nutrient loading to surface waters and improving water quality in these areas.

REFERENCES

Alyamani, M.S., and Z. Sen. 1993. Determination of hydraulic conductivity from complete grain-size distribution curves. *Ground Water* 31(4):551-555.

Andersen, H.E., and B. Kronvang. 2006. Modifying and evaluating a P index for Denmark. *Water Air and Soil Pollution* 174(1-4): 341-353.

Beauchemin, S. and R.R. Simard. 1999. Soil phosphorus saturation degree: Review of some indices and their suitability for P management in Quebec, Canada. *Canadian Journal of Soil Science* 79: 615-625.

Carlyle, G.C., and A.R. Hill. 2001. Groundwater phosphate dynamics in a river riparian zone: Effects of hydrologic flow paths, lithology, and redox chemistry. *Journal of Hydrology* 247: 151-168.

Cooper, A.B., C.M Smith, and M.J. Smith. 1995. Effects of riparian set-aside on soil characteristics in an agricultural landscape: Implications for nutrient transport and retention. *Agricultural Ecosystems Environment* 55: 61-67.

Daniel, T.C., A.N. Sharpley, and J.L. Lemunyon. 1998. Agricultural phosphorus and eutrophication: A symposium overview. *Journal of Environmental Quality* 27:251-257.

DeSutter, T.M., G.M. Pierzynski, and L.R. Baker. 2006. Flow through and batch methods for determining calcium-magnesium and magnesium-calcium selectivity. *Soil Science of America Journal* 70:550-554.

de Jonge, L.W., C. Kjaergaard, and P. Moldrup. 2004. Colloids and Colloid-Facilitated Transport of Contaminants in Soils: An Introduction. *Vadose Zone Journal* 3: 321-325.

Das, B.M. 2002. *Soil Mechanics Laboratory Manual.* 6th Edition, Oxford Unity Press, New York, NY.

Fuhrman, J. K., 1998. Phosphorus sorption and desorption characteristics of Oklahoma soils. M.S. Thesis, Oklahoma State University, Stillwater, OK.

Grant, R., A. Laubel, B. Kronvang, H. E. Anderson, L.M. Svendsen, and A. Fuglsang. 1996. Loss of dissolved particulate phosphorus from arable catchments by subsurface drainage. *Water Resources* 30: 2633-2642.

Heathwaite. L., P. Haygarth, R. Matthews, N. Preedy, and P. Butler. 2005. Evaluating colloidal phosphorus delivery to surface waters from diffuse agricultural sources. *Journal of Environmental Quality* 34 (1): 287-298.

Hively, W.D., P. Gerard-Marchant, and T.S. Steenhuis. 2006. Distributed hydrological modeling of total dissolved phosphorus transport in an agricultural landscape II. Dissolved phosphorus transport. *Hydrology and Earth System Sciences* 10(2): 263-276.

Hunt, B. 1978. Dispersive sources in uniform ground-water flow. *American Society of Civil Engineering Journal Hydraulics Division* 104(HY1): 75-85.

Ilg, K., and M. Kaupenjohann. 2005. Colloidal and dissolved phosphorus in sandy soils as affected by phosphorus saturation. *Journal of Environmental Quality* 34: 926-935.

Iyengar, S.S., L.W. Zelazny, and D.C. Martens. 1981. Effect of photolytic oxalate treatments on soil hydroxyl interlayered vermiculites. *Clays Clay Miner* 29: 429-434.

Kleinman, P.J.A., B.A. Needelman, A.N. Sharpley, and R.W. McDowell. 2004. Using soil phosphorus profile data to assess phosphorus leaching potential in manured soils. *Soil Science Society of America Journal* 67 (1): 215-224.

Landon, M. K., D. L. Rus, and F. E. Harvey. 2001. Comparison of instream methods for measuring hydraulic conductivity in sandy streambeds. *Ground Water* 39(6): 870-885.

Laubel, A., O.H. Jacobsen, B. Kronvang, R. Grant, and H.E. Anderson. 1999. Subsurface drainage loss of particles and phosphorus from field plot experiments and a tile-drained catchment. *Journal of Environmental Quality* 28: 576-584.

McCarty, G., and J. Angier. 2001. Impact of preferential flow pathways on ability of riparian wetlands to mitigate agricultural pollution. In Preferential Flow: Water Movement and Chemical Transport in the Environment, Proc. 2nd International Symposium. (3-5 January 2001, Honolulu, Hawaii. USA), eds David Bosch and Kevin King., St. Joseph, Michigan: American Society of Agricultural Engineers. pp 53-56.

McKeague, J. and J.H. Day. 1966. Diothionite and oxalate-extractable Fe and Al as aids in differentiating various classes of soils. *Canadian Journal of Soil Science* 46: 13-22.

Murphy, J., and J.R. Riley. 1962. A modified single solution method for the determination of phosphate in natural waters. *Analytica Chimica Acta* 27: 31-36.

Nelson, N.O., J.E. Parsons, and R.L. Mikkelson. 2005. Field-scale evaluation of phosphorus leaching in acid sandy soils receiving swine waste. *Journal of Environmental Quality* 34(6): 2024-2035.

Ogata, A. and R.B. Banks. 1961. A solution of the differential equation of longitudinal dispersion in porous media. *U.S. Geological Survey* Prof. Paper 411-A.

Osborne, L. L., and D.A. Kovacic. 1993. Riparian vegetated buffer strips in water-quality restoration and stream management. *Freshwater Biology* 29(2): 243-258.

Owens, L.B., and M.J. Shipitalo. 2006. Surface and subsurface phosphorus losses from fertilized pasture systems in Ohio. *Journal of Environmental Quality* 35: 1101-1109.

Polyakov, V., A. Fares, and M. H. Ryder. 2005. Precision riparian buffers for the control of nonpoint source pollutant loading into surface water: A review. *Environmental Review* 13: 129-144.

Pote, D.H., T.C. Daniel, A.N. Sharpley, P.A. Moore, Jr., D.R. Edwards, and D.J. Nichols. 1996. Relating extractable soil phosphorus to phosphorus losses in runoff. *Soil Science Society of America Journal* 60: 855-859.

Sauer, T.J., and S.D. Logsdon. 2002. Hydraulic and physical properties of stony soils in a small watershed. *Soil Science Society of America Journal* 66:1947–1956.

Storm D.E., White M.J., Smolen M.D., Zhang H. 2001. *Modeling Phosphorus Loading for the Lake Eucha Basin*. Submitted to the Tulsa Metropolitan Utility Authority, Department of Biosystems and Agricultural Engineering, Oklahoma State University, Stillwater, Oklahoma, May 22, 2001.

Storm, D.E., M.J. White, and M.D. Smolen. 2002. *Modeling the Lake Eucha Basin Using SWAT 2000*. Submitted to the Tulsa Metropolitan Utility Authority, Department of Biosystems and Agricultural Engineering, Oklahoma State University, Stillwater, Oklahoma, August 9, 2002.

Turner, B.L., and P.M. Haygarth. 2000. Phosphorus forms and concentrations in leachate under four grassland soil types. *Soil Science Society of America Journal* 64 (3): 1090-1099.

Vanek, V. 1993. Transport of groundwater-borne phosphorus to Lake Bysjon, South Sweden. *Hydrobiologia* 251(1-3): 211-216.

Wagner K, Woodruff S. 1997. *Phase I Clean Lakes Project, Diagnostic and Feasibility Study of Lake Eucha.* Oklahoma Conservation Commission, Oklahoma City, OK.

APPENDIX

Sieve Analysis on gravel subsoil

1st Sample

Sieve No.	Sieve Opening (mm)	Soil + Sieve Mass (g)	Sieve Mass (g)	Soil Mass (g)	Percent Mass Retained on each sieve	Cumulative Percent Retained	Percent Finer
1"	25.4	676.7	582.74	93.96	9.57	9.57	90.43
3/4"	19.05	668.5	597.6	70.9	7.22	16.79	83.21
1/2"	12.7	652.2	534.2	118	12.02	28.81	71.19
3/8"	9.525	654.5	558.1	96.4	9.82	38.63	61.37
4	4.75	503.5	379.2	124.3	12.66	51.29	48.71
10	2	579.2	466.8	112.4	11.45	62.74	37.26
20	0.85	498.6	385	113.6	11.57	74.31	25.69
40	0.425	628.14	504.5	123.64	12.59	86.91	13.09
70	0.212	400.7	321.2	79.5	8.10	95.00	5.00
100	0.15	421.9	397.05	24.85	2.53	97.54	2.46
200	0.075	353.64	342.74	10.9	1.11	98.65	1.35
Pan	-	391.1	379.37	11.73	1.19	99.84	0.16

Pan Mass	288.2
Pan + Gravel (wet)	2000.94
Pan + Gravel (dry)	1899.62
Gravel	1611.42

2nd Sample

Sieve No.	Sieve Opening (mm)	Soil + Sieve Mass (g)	Sieve Mass (g)	Soil Mass (g)	Percent Mass Retained on each sieve	Cumulative Percent Retained	Percent Finer
4	4.75	1781.3	531.1	1250.2	77.58	77.58	22.42
10	2	603.7	467.2	136.5	8.47	86.05	13.95
20	0.85	460.5	384.9	75.6	4.69	90.75	9.25
40	0.425	565.2	504.2	61	3.79	94.53	5.47
70	0.212	374.2	320.8	53.4	3.31	97.85	2.15
200	0.075	367.7	342.7	25	1.55	99.40	0.60
Pan	-	387.9	378.7	9.2	0.57	99.97	0.03

Sample 1	267.7
Sample 2	276.3
Can mass	46.5

Date: November 16, 2007
Water levels prior to and during 2nd injection experiment

Piezometer	Time	Water Level (m)
A	14:40	3.49
A	11:52	3.48
B	14:41	3.54
B	11:52	3.53
C	14:42	3.57
C	11:52	3.555
D	14:43	3.61
D	11:53	3.59
E	14:44	3.555
E	11:56	3.55
F	14:45	3.655
F	11:56	3.645
G	14:46	3.59
G	11:55	3.58
H	14:47	3.6
H	11:55	3.585
I	14:48	3.57
I	11:54	3.56
J	14:49	3.52
J	11:54	3.5
K	14:51	3.52
K	11:57	3.515
L	14:50	3.485
L	11:53	3.475
M	14:52	3.57
M	11:57	3.565
N	14:39	3.565
N	11:59	3.56
P	14:53	3.46
P	11:58	3.45

*Note: Water level indicates distance from top of piezometer casing to water table.

Date: November 16, 2007
Water level in trench prior to and during 2nd injection experiment

Time	Trench Water Depth (m)
12:45	0.6
12:50	0.6
12:55	0.6
13:00	0.59
13:05	0.6
13:10	0.6
13:15	0.6
13:35	0.6
13:40	0.6
13:45	0.6
13:50	0.6
13:55	0.6
14:00	0.6
14:05	0.6
14:10	0.6
14:15	0.6
14:20	0.6
14:25	0.6
14:30	0.6
14:35	0.6
14:40	0.6
14:45	0.6
14:50	0.6
14:55	0.6
15:00	0.6
15:05	0.6
15:10	0.61
15:15	0.6
15:20	0.6
15:25	0.6
15:30	0.6
15:35	0.6
15:40	0.6
15:45	0.6
15:50	0.6
15:55	0.61
16:00	0.61

Date: August 18, 2007

Injection: Rhodamine @ 100 ppm for 60 min

Piezometer (Sample Depth)	Elapsed Time (min)	Rhodamine Concentration (ppb)
A (U)	20	31.8
A (U)	41	10.8
A (U)	76	5.8
A (U)	115	0.0
A (L)	20	30.8
A (L)	42	9.2
A (L)	75	17.2
A (L)	115	0.0
C (U)	6	0.0
C (U)	35	17.9
C (U)	64	24.4
C (U)	126	0.0
C (L)	7	9.5
C (L)	36	35.1
C (L)	65	12.5
C (L)	126	1.9
E (U)	21	53.6
E (U)	43	7.9
E (U)	77	2.9
E (U)	112	3.3
E (L)	21	32.0
E (L)	44	16.7
E (L)	77	5.5
E (L)	112	2.2
G (U)	11	35.2
G (U)	36	15.7
G (U)	68	3.8
G (U)	122	0.0
G (L)	12	23.3
G (L)	37	21.4
G (L)	69	142.2
G (L)	123	0.0
I (U)	10	23.2
I (U)	31	38.9
I (U)	133	115.1
I (L)	10	36.1
I (L)	31	59.8
I (L)	134	0.0
K (U)	25	5.4
K (U)	49	11.8
K (U)	144	6.0
K (L)	26	4.8
K (L)	50	17.6
K (L)	144	0.0
M (U)	23	27.1
M (U)	51	12.4
M (U)	146	0.0
M (L)	24	8.0
M (L)	52	9.3
M (L)	146	0.0
P (U)	14	12.6
P (U)	46	8.4
P (U)	150	295.0
P (L)	15	27.5
P (L)	47	9.0
P (L)	150	260.9

Piezometer & Sample Depth	Elapsed Time (min)	Rhodamine Concentration (ppb)
B (U)	18	20.9
B (U)	38	21.6
B (U)	72	10.1
B (U)	120	3.5
B (L)	19	24.2
B (L)	39	25.6
B (L)	72	3.5
B (L)	121	0.0
D (U)	5	3108.0
D (U)	32	6255.0
D (U)	60	6771.0
D (U)	131	1625.0
D (L)	5	6.3
D (L)	35	4132.0
D (L)	60	-
D (L)	131	101.1
F (U)	16	11.6
F (U)	40	15.0
F (U)	74	4.2
F (U)	116	0.0
F (L)	17	32.5
F (L)	40	11.0
F (L)	74	8.2
F (L)	120	0.0
H (U)	11	0.0
H (U)	33	49.9
H (U)	61	17.2
H (U)	129	6.3
H (L)	11	15.2
H (L)	33	25.8
H (L)	62	16.2
H (L)	129	0.0
J (U)	8	5440.0
J (U)	29	7035.0
J (U)	137	184.8
J (L)	9	25.2
J (L)	30	14.1
L (U)	27	2.7
L (U)	48	7.8
L (U)	142	0.6
L (L)	27	7.3
L (L)	48	51.8
L (L)	143	0.0
N (U)	22	18.7
N (U)	44	69.5
N (U)	78	19.8
N (U)	110	7.9
N (L)	21	19.8
N (L)	45	16.7
N (L)	78	6.3
N (L)	111	1.6

Date: November 16, 2007
Injection: Rhodamine @ 3.0 ppm for 90 min & Phosphorus @ 100 ppm for 90 min

Started Injection	Stopped Injection
12:36	14:06:27

Sample #	Time	Elapsed Time	Well	Location	Rhodamine Concentration (ppb)	Phosphorus Concentration (ppm)
1	12:37	0:01	Trench		589	17.7
2	12:40	0:04	Trench		2911	77.6
3	12:44	0:08	Trench		2914	94.7
4	12:50	0:14	Trench		3778	114
5	13:01	0:25	Trench		3214	122
6	13:09	0:33	Trench		4425	91.1
7	13:17	0:41	Trench		3569	129
8	13:22	0:46	Trench		3708	111
9	13:31	0:55	Trench		3529	117
10	13:39	1:03	Trench		2956	120
11	13:46	1:10	Trench		1900	71.3
12	14:05	1:29	Trench		1862	69.4
13	14:16	1:40	Trench		2282	7.23
14	14:25	1:49	Trench		27.35	1.01
15	14:41	2:05	Trench		7.958	0.0917
16	14:54	2:18	Trench		0.457	0.0435
17	15:08	2:32	Trench		5.365	0.0419
18	15:56	3:20	Trench		0	0.0417
19		Backgrounc	Creek		5.182	0.0891
20		Backgrounc	A	TOP (BG)	1.839	0.0449
21	12:40	0:04	A	TOP	2.225	0.0377
22	12:52	0:16	A	TOP	0.866	0.046
23	13:04	0:28	A	TOP	5.354	0.0433
24	13:18	0:42	A	TOP	3.921	0.108
25	13:32	0:56	A	TOP	5.799	0.0588
26	13:58	1:22	A	TOP	0.777	0.0309
27	14:17	1:41	A	TOP	1.448	0.0383
28	14:44	2:08	A	TOP	3.122	0.0792
29		Backgrounc	A	BOTTOM (BG)	4.903	0.0454
30	12:40	0:04	A	BOTTOM	4.197	0.0429
31	12:52	0:16	A	BOTTOM	0.66	0.0478
32	13:04	0:28	A	BOTTOM	4.169	0.0438
33	13:18	0:42	A	BOTTOM	1.268	0.0487
34	13:32	0:56	A	BOTTOM	2.085	0.0637
35	13:58	1:22	A	BOTTOM	6.69	0.0711
36	14:17	1:41	A	BOTTOM	0.043	0.0395
37	14:44	2:08	A	BOTTOM	4.598	0.124
38		Backgrounc	B	TOP (BG)	4.914	0.0462
39	12:42	0:06	B	TOP	1.465	0.035
40	12:53	0:17	B	TOP	0.4	0.0445
41	13:05	0:29	B	TOP	0	0.042
42	13:19	0:43	B	TOP	0	0.0701
43	13:32	0:56	B	TOP	0.097	0.072
44	14:18	1:42	B	TOP	6.856	0.0479
45	14:48	2:12	B	TOP	0.812	0.0474
46	15:45	3:09	B	BOTTOM	0.542	0.0494
47		Backgrounc	B	BOTTOM (BG)	0	0.0442
48	12:42	0:06	B	BOTTOM	0	0.0426
49	12:53	0:17	B	BOTTOM	1.107	0.0445
50	13:05	0:29	B	BOTTOM	0	0.0591
51	13:19	0:43	B	BOTTOM	0.234	0.0514
52	13:32	0:56	B	BOTTOM	0	0.0463
53	14:17	1:41	B	BOTTOM	0	0.0438
54	14:46	2:10	B	BOTTOM	0.206	0.064
55	15:45	3:09	B	TOP	1.553	0.0529

56		Backgrounc	C	TOP (BG)	0.636	0.0459
57	12:43	0:07	C	TOP	0.85	0.0385
58	12:54	0:18	C	TOP	0.074	0.0426
59	13:06	0:30	C	TOP	2.08	0.0456
60	13:19	0:43	C	TOP	1.998	0.124
61	13:33	0:57	C	TOP	0	0.0456
62	13:59	1:23	C	TOP	6.781	0.0593
63	14:19	1:43	C	TOP	0	0.047
64	14:47	2:11	C	TOP	1.911	0.0495
65	15:46	3:10	C	TOP	0.755	0.0463
66		Backgrounc	C	BOTTOM (BG)	0	0.0452
67	12:43	0:07	C	BOTTOM	0	0.0408
68	12:53	0:17	C	BOTTOM	0.416	0.0442
69	13:06	0:30	C	BOTTOM	0	0.0444
70	13:19	0:43	C	BOTTOM	1.319	0.0519
71	13:33	0:57	C	BOTTOM	0	0.0456
72	13:59	1:23	C	BOTTOM	0.473	0.0313
73	14:19	1:43	C	BOTTOM	0	0.0448
74	14:47	2:11	C	BOTTOM	0.825	0.0476
75	15:46	3:10	C	BOTTOM	0.715	0.0557
76		Backgrounc	D	TOP (BG)	0.577	0.0498
77	12:44	0:08	D	TOP	3.45	0.0293
78	12:54	0:18	D	TOP	1610	50.5
79	13:07	0:31	D	TOP	1700	50.3
80	13:20	0:44	D	TOP	3070	106
81	13:35	0:59	D	TOP	2889	106
82	14:00	1:24	D	TOP	2344	114
83	14:21	1:45	D	TOP	1059	39.2
84	14:29	1:53	D	TOP	308.7	9.25
85	15:47	3:11	D	TOP	166.5	3.15
86		Backgrounc	D	BOTTOM (BG)	0.423	0.0536
87	12:43	0:07	D	BOTTOM	5.246	0.0303
88	12:54	0:18	D	BOTTOM	24.81	0.841
89	13:07	0:31	D	BOTTOM	7.579	0.131
90	13:20	0:44	D	BOTTOM	386.9	11.3
91	13:35	0:59	D	BOTTOM	122.2	4.07
92	14:00	1:24	D	BOTTOM	389.3	16.8
93	14:21	1:45	D	BOTTOM	35.94	1.18
94	14:49	2:13	D	BOTTOM	19.14	0.462
95	15:47	3:11	D	BOTTOM	10.05	0.125
96		Backgrounc	E	TOP (BG)	2.482	0.0484
97	12:45	0:09	E	TOP	0	0.0486
98	12:55	0:19	E	TOP	1.907	0.0464
99	13:10	0:34	E	TOP	0.876	0.0481
100	13:23	0:47	E	TOP	1.666	0.0475
101	14:26	1:50	E	TOP	4.481	0.0377
102	14:56	2:20	E	TOP	2.536	0.0494
103	15:48	3:12	E	TOP	0.088	0.045
104		Backgrounc	E	BOTTOM (BG)	0.944	0.0481
105	12:44	0:08	E	BOTTOM	2.05	0.0477
106	12:55	0:19	E	BOTTOM	1.984	0.0563
107	13:10	0:34	E	BOTTOM	0.818	0.0515
108	13:23	0:47	E	BOTTOM	1.451	0.0503
109	14:26	1:50	E	BOTTOM	0.466	0.0364
110	14:56	2:20	E	BOTTOM	1.999	0.0616
111	15:48	3:12	E	BOTTOM	0.466	0.108

112		Backgrounc	F	TOP (BG)	27.42	0.128
113	12:56	0:20	F	TOP	0.996	0.0434
114	13:11	0:35	F	TOP	4.523	0.0775
115	13:24	0:48	F	TOP	0.198	0.0444
116	14:02	1:26	F	TOP	4.087	0.05
117	14:57	2:21	F	TOP	0.767	0.0437
118	15:48	3:12	F	TOP	0.543	0.0458
119		Backgrounc	F	BOTTOM (BG)	0.215	0.0475
120	12:45	0:09	F	BOTTOM	0	0.0474
121	12:56	0:20	F	BOTTOM	0.437	0.0442
122	13:11	0:35	F	BOTTOM	0.89	0.0452
123	13:24	0:48	F	BOTTOM	0.263	0.0525
124	14:02	1:26	F	BOTTOM	2.087	0.0448
125	14:57	2:21	F	BOTTOM	4.876	0.0474
126	15:48	3:12	F	BOTTOM	0	0.0458
127		Backgrounc	G	TOP (BG)	0.026	0.0462
128	12:47	0:11	G	TOP	0	0.0435
129	12:57	0:21	G	TOP	1.439	0.0459
130	13:12	0:36	G	TOP	0.168	0.0462
131	13:25	0:49	G	TOP	0	0.0488
132	14:03	1:27	G	TOP	1.473	0.111
133	14:28	1:52	G	TOP	0.048	0.053
134	14:59	2:23	G	TOP	0.138	0.046
135	15:49	3:13	G	TOP	0	0.0449
136		Backgrounc	G	TOP (BG)	0	0.0472
137	12:46	0:10	G	TOP	1.926	0.0447
138	12:57	0:21	G	TOP	4.757	0.0457
139	13:12	0:36	G	TOP	2.536	0.0493
140	13:25	0:49	G	TOP	0.804	0.0473
141	14:03	1:27	G	TOP	0	0.0495
142	14:28	1:52	G	TOP	0.593	0.0324
143	14:59	2:23	G	TOP	0	0.0427
144	15:49	3:13	G	TOP	0.248	0.0464
145		Backgrounc	H	TOP (BG)	2.089	0.0491
146	12:48	0:12	H	TOP	0	0.046
147	12:58	0:22	H	TOP	0	0.0502
148	13:13	0:37	H	TOP	1.778	0.0445
149	13:26	0:50	H	TOP	0	0.0521
150	14:04	1:28	H	TOP	1.689	0.0881
151	15:00	2:24	H	TOP	0	0.0911
152	15:51	3:15	H	TOP	4.406	0.0482
153		Backgrounc	H	BOTTOM (BG)	0	0.0475
154	12:48	0:12	H	BOTTOM	0.184	0.0424
155	12:58	0:22	H	BOTTOM	1.019	0.0457
156	13:13	0:37	H	BOTTOM	0.819	0.0449
157	13:26	0:50	H	BOTTOM	1.148	0.0498
158	14:04	1:28	H	BOTTOM	0.136	0.0384
159	15:00	2:24	H	BOTTOM	2.078	0.0638
160	15:51	3:15	H	BOTTOM	0.819	0.105
161		Backgrounc	I	TOP (BG)	4.096	0.054
162	12:49	0:13	I	TOP	0	0.0455
163	12:39	0:03	I	TOP	4.34	0.0377
164	12:58	0:22	I	TOP	22.72	0.739
165	13:14	0:38	I	TOP	180.6	6.04
166	13:26	0:50	I	TOP	315.6	12.2
167	14:30	1:54	I	TOP	350.3	10.4
168	15:02	2:26	I	TOP	192	5.46
169	15:51	3:15	I	TOP	127.2	2.25
170		Backgrounc	I	BOTTOM (BG)	5.372	0.0475
171	12:49	0:13	I	BOTTOM	0.499	0.0488
172	12:39	0:03	I	BOTTOM	4.044	0.0495
173	12:58	0:22	I	BOTTOM	0.404	0.0438
174	13:13	0:37	I	BOTTOM	5.75	0.0434
175	13:26	0:50	I	BOTTOM	0.373	0.0615
176	14:30	1:54	I	BOTTOM	5.001	0.0727
177	15:02	2:26	I	BOTTOM	0.604	0.0585
178	15:51	3:15	I	BOTTOM	5.597	0.0479

179		Backgrounc	J	TOP (BG)	0	0.0503
180	12:50	0:14	J	TOP	12.18	0.324
181	12:38	0:02	J	TOP	3.946	0.044
182	12:59	0:23	J	TOP	3540	97.2
183	13:08	0:32	J	TOP	1246	33.5
184	13:21	0:45	J	TOP	3790	116
185	13:36	1:00	J	TOP	3284	113
186	14:22	1:46	J	TOP	2664	129
187	14:50	2:14	J	TOP	108.2	1.87
188	15:52	3:16	J	TOP	4.159	1.15
189		Backgrounc	J	BOTTOM (BG)	0	0.0485
190	12:50	0:14	J	BOTTOM	3.854	0.0457
191	12:38	0:02	J	BOTTOM	0	0.0433
192	12:59	0:23	J	BOTTOM	5.334	0.0749
193	13:08	0:32	J	BOTTOM	33.02	1.06
194	13:21	0:45	J	BOTTOM	37.06	1.19
195	13:36	1:00	J	BOTTOM	66.42	2.19
196	14:22	1:46	J	BOTTOM	46.18	1.74
197	14:50	2:14	J	BOTTOM	0.656	0.059
198	15:52	3:16	J	BOTTOM	4.444	0.0357
199		Backgrounc	K	TOP (BG)	0	0.0467
200	13:02	0:26	K	TOP	0	0.0449
201	13:17	0:41	K	TOP	0	0.046
202	13:30	0:54	K	TOP	0	0.0422
203	14:07	1:31	K	TOP	0	0.0417
204	14:33	1:57	K	TOP	0	0.0652
205	15:05	2:29	K	TOP	0	0.0419
206	15:03	2:27	K	TOP	0.739	0.046
207		Backgrounc	K	BOTTOM (BG)	0	0.0461
208	13:01	0:25	K	BOTTOM	3.41	0.0344
209	13:16	0:40	K	BOTTOM	0	0.0448
210	13:30	0:54	K	BOTTOM	0	0.034
211	14:07	1:31	K	BOTTOM	0.478	0.0403
212	14:33	1:57	K	BOTTOM	4.366	0.053
213	15:04	2:28	K	BOTTOM	0.203	0.048
214	15:53	3:17	K	BOTTOM	0	0.0394
215		Backgrounc	L	TOP (BG)	5.12	0.0468
216	13:03	0:27	L	TOP	0.114	0.0396
217	13:15	0:39	L	TOP	0	0.0441
218	13:27	0:51	L	TOP	5.354	0.032
219	14:08	1:32	L	TOP	5.239	0.0395
220	14:32	1:56	L	TOP	5.196	0.0662
221	15:03	2:27	L	TOP	0	0.0422
222	15:54	3:18	L	TOP	0.49	0.0504
223		Backgrounc	L	BOTTOM (BG)	0.423	0.0446
224	13:03	0:27	L	BOTTOM	6.203	0.0359
225	13:15	0:39	L	BOTTOM	5.122	0.0432
226	13:27	0:51	L	BOTTOM	0.961	0.0319
227	14:08	1:32	L	BOTTOM	1.333	0.0494
228	14:31	1:55	L	BOTTOM	0	0.0297
229	15:03	2:27	L	BOTTOM	5.975	0.042
230	15:54	3:18	L	BOTTOM	5.123	0.0481
231		Backgrounc	N	TOP (BG)	6.244	0.0474
232	12:51	0:15	N	TOP	0.073	0.0433
233	13:00	0:24	N	TOP	6.329	0.0422
234	13:09	0:33	N	TOP	1.101	0.0422
235	13:22	0:46	N	TOP	6.891	0.0524
236	13:37	1:01	N	TOP	2.76	0.101
237	14:24	1:48	N	TOP	6.154	0.0442
238	14:53	2:17	N	TOP	6.67	0.0465
239	15:56	3:20	N	TOP	0	0.0432
240		Backgrounc	N	BOTTOM (BG)	5.738	0.0426
241	12:51	0:15	N	BOTTOM	0.881	0.0288
242	13:00	0:24	N	BOTTOM	10.11	0.0579
243	13:09	0:33	N	BOTTOM	26.38	0.0429
244	13:22	0:46	N	BOTTOM	0.263	0.041
245	13:37	1:01	N	BOTTOM	5.45	0.0478
246	14:24	1:48	N	BOTTOM	1.443	0.0445
247	14:53	2:17	N	BOTTOM	8.25	0.0436
248	15:55	3:19	N	BOTTOM	0.408	0.0664

249		Backgrounc	M	BOTTOM (BG)	5.091	0.0478
250	13:03	0:27	M	TOP	4.662	0.0605
251	13:16	0:40	M	TOP	6.348	0.039
252	13:29	0:53	M	TOP	0.205	0.0552
253	14:34	1:58	M	TOP	0	0.0477
254	15:06	2:30	M	TOP	0	0.0479
255	15:55	3:19	M	TOP	5.937	0.0451
256		Backgrounc	M	TOP (BG)	0	0.0511
257	13:03	0:27	M	BOTTOM	5.501	0.0819
258	13:16	0:40	M	BOTTOM	0	0.0547
259	13:29	0:53	M	BOTTOM	0.684	0.0344
260	14:34	1:58	M	BOTTOM	0	0.0351
261	15:06	2:30	M	BOTTOM	0	0.0929
262	15:55	3:19	M	BOTTOM	5.554	0.0424

Sample #	Piezometer	Time	Elapsed Time	MR-P (ppm)	ICP-P (ppm)	Ca (ppm)	Fe (ppm)	Al (ppm)
1	Trench	12:37	0:01	17.70	40.30	87.61	0.01	0.02
2	Trench	12:40	0:04	77.60	65.90	79.13	0.01	0.05
3	Trench	12:44	0:08	94.70	50.50	79.31	0.01	0.07
4	Trench	12:50	0:14	114.00	56.10	85.15	0.02	0.08
5	Trench	13:01	0:25	122.00	65.60	76.62	0.01	0.09
6	Trench	13:09	0:33	91.10	83.30	84.87	0.00	0.06
7	Trench	13:17	0:41	129.00	129.00	72.40	0.00	0.10
8	Trench	13:22	0:46	111.00	115.70	72.65	0.01	0.08
9	Trench	13:31	0:55	117.00	98.60	73.97	0.01	0.08
10	Trench	13:39	1:03	120.00	112.20	93.43	0.02	0.10
11	Trench	13:46	1:10	71.30	75.80	56.65	0.01	0.05
12	Trench	14:05	1:29	69.40	66.00	70.10	0.01	0.05
13	Trench	14:16	1:40	7.23	7.69	39.97	0.00	0.01
14	Trench	14:25	1:49	1.01	0.97	39.63	0.01	0.00
15	Trench	14:41	2:05	0.09	0.05	34.63	0.00	0.00
16	Trench	14:54	2:18	0.04	0.02	38.29	0.00	0.00
17	Trench	15:08	2:32	0.04	0.02	39.42	0.01	0.00
18	Trench	15:56	3:20	0.04	0.03	38.92	0.00	0.00
19	Creek		Backgrounc	0.09	0.05	39.65	0.00	0.00
20	A		Backgrounc	0.04	0.01	38.04	0.00	0.00
21	A	12:40	0:04	0.04	0.02	37.82	0.00	0.08
22	A	12:52	0:16	0.05	0.01	39.19	0.11	0.20
23	A	13:04	0:28	0.04	0.02	38.45	0.01	0.02
24	A	13:18	0:42	0.11	0.08	37.49	0.01	0.00
25	A	13:32	0:56	0.06	0.00	38.11	0.00	0.00
26	A	13:58	1:22	0.03	0.01	43.52	0.01	0.00
27	A	14:17	1:41	0.04	0.02	42.17	0.00	0.01
28	A	14:44	2:08	0.08	0.07	32.43	0.00	0.00
29	A		Backgrounc	0.05	0.00	38.23	0.00	0.00
30	A	12:40	0:04	0.04	0.01	39.67	0.00	0.07
31	A	12:52	0:16	0.05	0.00	38.07	0.00	0.00
32	A	13:04	0:28	0.04	0.01	37.63	0.00	0.00
33	A	13:18	0:42	0.05	0.02	37.29	0.00	0.01
34	A	13:32	0:56	0.06	0.00	37.91	0.00	0.00
35	A	13:58	1:22	0.07	0.04	39.61	0.01	0.00
36	A	14:17	1:41	0.04	0.02	38.86	0.00	0.00
37	A	14:44	2:08	0.12	0.11	26.40	0.00	0.01
38	B		Backgrounc	0.05	0.01	38.39	0.00	0.00
39	B	12:42	0:06	0.04	0.03	40.11	0.01	0.01
40	B	12:53	0:17	0.04	0.00	39.75	0.01	0.02
41	B	13:05	0:29	0.04	0.00	39.99	0.00	0.00
42	B	13:19	0:43	0.07	0.03	39.69	0.00	0.00
43	B	13:32	0:56	0.07	0.02	39.60	0.00	0.00
44	B	14:18	1:42	0.05	0.02	39.81	0.00	0.07
45	B	14:48	2:12	0.05	0.01	37.73	0.00	0.01
46	B	15:45	3:09	0.05	0.01	38.76	0.00	0.00
47	B		Backgrounc	0.04	0.01	39.67	0.00	0.00
48	B	12:42	0:06	0.04	0.01	41.33	0.00	0.10
49	B	12:53	0:17	0.04	0.01	39.41	0.00	0.01
50	B	13:05	0:29	0.06	0.02	38.75	0.04	0.07
51	B	13:19	0:43	0.05	0.02	38.41	0.00	0.00
52	B	13:32	0:56	0.05	0.03	38.64	0.00	0.00
53	B	14:17	1:41	0.04	0.01	37.82	0.00	0.00
54	B	14:46	2:10	0.06	0.03	37.28	0.00	0.00
55	B	15:45	3:09	0.05	0.02	38.12	0.00	0.00
56	C		Backgrounc	0.05	0.00	40.22	0.00	0.00
57	C	12:43	0:07	0.04	0.00	40.81	0.01	0.14
58	C	12:54	0:18	0.04	0.03	40.49	0.04	0.09
59	C	13:06	0:30	0.05	0.00	40.24	0.01	0.02
60	C	13:19	0:43	0.12	0.08	40.30	0.10	0.17
61	C	13:33	0:57	0.05	0.01	39.90	0.00	0.00
62	C	13:59	1:23	0.06	0.02	42.03	0.02	0.07
63	C	14:19	1:43	0.05	0.00	39.87	0.01	0.05
64	C	14:47	2:11	0.05	0.03	37.81	0.09	0.19
65	C	15:46	3:10	0.05	0.00	40.16	0.08	0.15
66	C		Backgrounc	0.05	0.00	39.53	0.00	0.00
67	C	12:43	0:07	0.04	0.00	40.48	0.01	0.13
68	C	12:53	0:17	0.04	0.01	40.54	0.00	0.01
69	C	13:06	0:30	0.04	0.01	40.13	0.01	0.02
70	C	13:19	0:43	0.05	0.01	40.55	0.03	0.07
71	C	13:33	0:57	0.05	0.03	39.68	0.01	0.01
72	C	13:59	1:23	0.03	0.00	40.48	0.00	0.02
73	C	14:19	1:43	0.04	0.01	39.91	0.01	0.03
74	C	14:47	2:11	0.05	0.04	37.19	0.02	0.05
75	C	15:46	3:10	0.06	0.05	39.78	0.04	0.07

76	D		Backgound	0.05	0.02	39.71	0.00	0.01
77	D	12:44	0:08	0.03	0.01	40.75	0.00	0.02
78	D	12:54	0:18	50.50	54.90	83.01	0.07	0.09
79	D	13:07	0:31	50.30	56.50	76.13	0.09	0.14
80	D	13:20	0:44	106.00	89.20	99.57	0.07	0.06
81	D	13:35	0:59	106.00	98.40	111.64	0.13	0.18
82	D	14:00	1:24	114.00	95.30	97.05	0.08	0.06
83	D	14:21	1:45	39.20	38.15	74.92	0.06	0.11
84	D	14:29	1:53	9.25	20.30	80.18	0.07	0.13
85	D	15:47	3:11	3.15	6.69	76.03	0.08	0.14
86	D		Backgound	0.05	0.01	38.52	0.01	0.01
87	D	12:43	0:07	0.03	0.01	41.31	0.00	0.02
88	D	12:54	0:18	0.84	0.79	39.01	0.01	0.02
89	D	13:07	0:31	0.13	0.08	38.98	0.00	0.01
90	D	13:20	0:44	11.30	28.37	94.08	0.02	0.02
91	D	13:35	0:59	4.07	10.02	83.04	0.01	0.00
92	D	14:00	1:24	16.80	37.64	88.95	0.02	0.01
93	D	14:21	1:45	1.18	1.06	40.23	0.00	0.02
94	D	14:49	2:13	0.46	0.42	36.93	0.00	0.00
95	D	15:47	3:11	0.13	0.09	25.27	0.00	0.00
96	E		Backgound	0.05	0.00	38.92	0.00	0.01
97	E	12:45	0:09	0.05	0.05	39.92	0.00	0.00
98	E	12:55	0:19	0.05	0.03	40.15	0.01	0.02
99	E	13:10	0:34	0.05	0.03	40.27	0.00	0.01
100	E	13:23	0:47	0.05	0.01	40.37	0.00	0.00
101	E	14:26	1:50	0.04	0.00	39.64	0.00	0.00
102	E	14:56	2:20	0.05	0.01	38.82	0.01	0.01
103	E	15:48	3:12	0.05	0.01	40.49	0.00	0.01
104	E		Backgound	0.05	0.00	39.29	0.01	0.02
105	E	12:44	0:08	0.05	0.01	39.25	0.06	0.13
106	E	12:55	0:19	0.06	0.01	39.66	0.17	0.34
107	E	13:10	0:34	0.05	0.02	39.89	0.37	0.71
108	E	13:23	0:47	0.05	0.03	39.52	0.01	0.01
109	E	14:26	1:50	0.04	0.00	39.44	0.00	0.00
110	E	14:56	2:20	0.06	0.02	38.30	0.02	0.04
111	E	15:48	3:12	0.11	0.07	39.66	0.03	0.06
112	F		Backgound	0.13	-	-	-	-
113	F	12:56	0:20	0.04	0.03	41.94	0.00	0.00
114	F	13:11	0:35	0.08	0.09	41.27	0.00	0.00
115	F	13:24	0:48	0.04	0.02	41.05	0.00	0.00
116	F	14:02	1:26	0.05	0.05	41.03	0.01	0.00
117	F	14:57	2:21	0.04	0.03	40.96	0.00	0.00
118	F	15:48	3:12	0.05	0.00	41.68	0.00	0.00
119	F		Backgound	0.05	0.03	40.82	0.00	0.00
120	F	12:45	0:09	0.05	0.03	40.86	0.01	0.00
121	F	12:56	0:20	0.04	0.04	42.20	0.01	0.01
122	F	13:11	0:35	0.04	0.03	41.16	0.01	0.01
123	F	13:24	0:48	0.05	0.02	41.79	0.00	0.00
124	F	14:02	1:26	0.05	0.03	41.92	0.01	0.00
125	F	14:57	2:21	0.05	0.04	41.10	0.01	0.01
126	F	15:48	3:12	0.05	0.04	41.92	0.00	0.00
127	G		Backgound	0.05	0.04	41.08	0.01	0.00
128	G	12:47	0:11	0.04	0.04	40.69	0.00	0.00
129	G	12:57	0:21	0.05	0.03	41.98	0.00	0.00
130	G	13:12	0:36	0.05	0.03	40.79	0.01	0.00
131	G	13:25	0:49	0.05	0.03	41.49	0.00	0.00
132	G	14:03	1:27	0.11	0.07	42.60	0.01	0.01
133	G	14:28	1:52	0.05	0.04	41.24	0.01	0.00
134	G	14:59	2:23	0.05	0.00	41.50	0.00	0.00
135	G	15:49	3:13	0.04	0.02	40.98	0.01	0.00
136	G		Backgound	0.05	0.04	42.05	0.01	0.00
137	G	12:46	0:10	0.04	0.04	41.73	0.00	0.00
138	G	12:57	0:21	0.05	0.02	41.27	0.01	0.00
139	G	13:12	0:36	0.05	0.04	41.54	0.00	0.00
140	G	13:25	0:49	0.05	0.02	40.76	0.00	0.00
141	G	14:03	1:27	0.05	0.02	43.20	0.00	0.00
142	G	14:28	1:52	0.03	0.01	41.30	0.01	0.00
143	G	14:59	2:23	0.04	0.02	41.55	0.01	0.00
144	G	15:49	3:13	0.05	0.04	41.42	0.00	0.00

145	H		Backgrounc	0.05	0.04	41.46	0.01	0.00
146	H	12:48	0:12	0.05	0.02	42.19	0.01	0.00
147	H	12:58	0:22	0.05	0.07	42.40	0.01	0.01
148	H	13:13	0:37	0.04	0.02	42.01	0.00	0.00
149	H	13:26	0:50	0.05	0.06	42.16	0.00	0.00
150	H	14:04	1:28	0.09	0.09	43.54	0.01	0.00
151	H	15:00	2:24	0.09	0.02	40.71	0.01	0.00
152	H	15:51	3:15	0.05	0.04	41.86	0.00	0.00
153	H		Backgrounc	0.05	0.00	42.50	0.00	0.00
154	H	12:48	0:12	0.05	0.03	42.45	0.00	0.00
155	H	12:58	0:22	0.04	0.03	40.97	0.00	0.00
156	H	13:13	0:37	0.04	0.04	43.18	0.01	0.01
157	H	13:26	0:50	0.05	0.02	42.18	0.01	0.00
158	H	14:04	1:28	0.04	0.02	43.92	0.01	0.01
159	H	15:00	2:24	0.06	0.05	39.63	0.01	0.00
160	H	15:51	3:15	0.11	0.07	41.63	0.00	0.00
161	I		Backgrounc	0.05	0.04	42.42	0.01	0.00
162	I	12:49	0:13	0.05	0.02	41.54	0.01	0.00
163	I	12:39	0:03	0.04	0.03	41.12	0.01	0.00
164	I	12:58	0:22	0.74	0.68	41.65	0.01	0.01
165	I	13:14	0:38	0.04	0.05	41.59	0.01	0.00
166	I	13:26	0:50	12.20	26.91	87.00	0.04	0.05
167	I	14:30	1:54	10.40	22.24	88.65	0.00	0.02
168	I	15:02	2:26	5.46	11.34	91.58	0.02	0.01
169	I	15:51	3:15	0.05	0.02	41.40	0.00	0.00
170	I		Backgrounc	0.05	0.02	42.28	0.01	0.00
171	I	12:49	0:13	0.05	0.05	41.73	0.00	0.00
172	I	12:39	0:03	0.05	0.01	41.69	0.01	0.01
173	I	12:58	0:22	0.04	0.01	40.94	0.01	0.00
174	I	13:13	0:37	6.04	11.63	71.75	0.08	0.15
175	I	13:26	0:50	0.06	0.03	41.15	0.01	0.00
176	I	14:30	1:54	0.07	0.06	41.23	0.00	0.00
177	I	15:02	2:26	0.06	0.06	38.19	0.00	0.00
178	I	15:51	3:15	2.25	2.44	38.01	0.02	0.03
179	J		Backgrounc	0.05	0.01	38.04	0.00	0.00
180	J	12:50	0:14	0.32	0.28	37.39	0.03	0.06
181	J	12:38	0:02	0.04	0.01	37.58	0.00	0.00
182	J	12:59	0:23	97.20	90.00	92.15	0.07	0.06
183	J	13:08	0:32	33.50	30.78	72.75	0.05	0.05
184	J	13:21	0:45	116.00	99.20	77.61	0.08	0.06
185	J	13:36	1:00	113.00	100.60	67.19	0.05	0.02
186	J	14:22	1:46	129.00	116.10	71.69	0.02	0.06
187	J	14:50	2:14	1.87	1.75	32.64	0.01	0.01
188	J	15:52	3:16	1.15	1.12	26.98	0.00	0.01
189	J		Backgrounc	0.05	0.02	37.15	0.00	0.00
190	J	12:50	0:14	0.05	0.02	37.59	0.00	0.00
191	J	12:38	0:02	0.04	0.00	36.66	0.00	0.00
192	J	12:59	0:23	0.07	-	-	-	-
193	J	13:08	0:32	1.06	0.95	38.49	0.00	0.00
194	J	13:21	0:45	1.19	1.10	37.50	0.00	0.00
195	J	13:36	1:00	2.19	3.08	59.91	0.01	0.02
196	J	14:22	1:46	1.74	1.57	37.03	0.00	0.00
197	J	14:50	2:14	0.06	0.03	34.59	0.00	0.00
198	J	15:52	3:16	0.04	0.01	30.58	0.00	0.00
199	K		Backgrounc	0.05	0.00	41.82	0.00	0.00
200	K	13:02	0:26	0.04	0.02	42.88	0.01	0.00
201	K	13:17	0:41	0.05	0.01	41.68	0.00	0.00
202	K	13:30	0:54	0.04	0.04	40.91	0.01	0.00
203	K	14:07	1:31	0.04	0.04	43.37	0.00	0.00
204	K	14:33	1:57	0.07	0.06	41.50	0.01	0.00
205	K	15:05	2:29	0.04	0.00	42.23	0.01	0.00
206	K	15:03	2:27	0.05	0.02	41.86	0.01	0.00
207	K		Backgrounc	0.05	0.06	41.88	0.01	0.01
208	K	13:01	0:25	0.03	0.04	41.69	0.01	0.00
209	K	13:16	0:40	0.04	0.02	42.62	0.00	0.00
210	K	13:30	0:54	0.03	0.00	41.76	0.01	0.01
211	K	14:07	1:31	0.04	0.03	42.83	0.00	0.00
212	K	14:33	1:57	0.05	0.04	41.85	0.01	0.01
213	K	15:04	2:28	0.05	0.00	40.55	0.00	0.00
214	K	15:53	3:17	0.04	0.04	40.76	0.00	0.00

215	L		Backgrounc	0.05	0.01	42.18	0.01	0.01
216	L	13:03	0:27	0.04	0.03	41.25	0.00	0.00
217	L	13:15	0:39	0.04	0.05	40.77	0.01	0.00
218	L	13:27	0:51	0.03	0.04	40.81	0.01	0.01
219	L	14:08	1:32	0.04	0.03	43.00	0.00	0.01
220	L	14:32	1:56	0.07	0.04	40.60	0.01	0.00
221	L	15:03	2:27	0.04	0.01	41.51	0.00	0.00
222	L	15:54	3:18	0.05	0.05	39.19	0.00	0.00
223	L		Backgrounc	0.04	0.00	41.00	0.01	0.01
224	L	13:03	0:27	0.04	0.05	42.04	0.01	0.02
225	L	13:15	0:39	0.04	0.06	41.64	0.01	0.01
226	L	13:27	0:51	0.03	0.02	40.61	0.01	0.01
227	L	14:08	1:32	0.05	0.01	43.63	0.00	0.00
228	L	14:31	1:55	0.03	0.03	41.71	0.01	0.01
229	L	15:03	2:27	0.04	0.02	40.81	0.00	0.00
230	L	15:54	3:18	0.05	0.03	40.90	0.02	0.03
231	N		Backgrounc	0.05	0.03	71.75	0.16	0.26
232	N	12:51	0:15	0.04	0.06	64.40	0.01	0.01
233	N	13:00	0:24	0.04	0.04	66.33	0.01	0.00
234	N	13:09	0:33	0.04	0.08	69.79	0.01	0.00
235	N	13:22	0:46	0.05	0.02	66.22	0.02	0.03
236	N	13:37	1:01	0.10	0.06	69.68	0.02	0.01
237	N	14:24	1:48	0.04	0.02	75.67	0.01	0.01
238	N	14:53	2:17	0.05	0.06	62.25	0.00	0.00
239	N	15:56	3:20	0.04	0.05	49.99	0.00	0.01
240	N		Backgrounc	0.04	0.05	67.66	0.06	0.11
241	N	12:51	0:15	0.03	0.03	68.47	0.05	0.07
242	N	13:00	0:24	0.06	0.04	69.44	0.12	0.28
243	N	13:09	0:33	0.04	0.07	73.04	0.10	0.23
244	N	13:22	0:46	0.04	0.05	76.45	0.12	0.24
245	N	13:37	1:01	0.05	0.02	78.26	0.02	0.02
246	N	14:24	1:48	0.04	0.03	72.53	0.04	0.09
247	N	14:53	2:17	0.04	0.12	55.96	0.01	0.00
248	N	15:55	3:19	0.07	0.04	53.90	0.01	0.00
249	M		Backgrounc	0.05	0.00	39.46	0.00	0.00
250	M	13:03	0:27	0.06	0.01	41.29	0.01	0.00
251	M	13:16	0:40	0.04	0.06	41.04	0.01	0.02
252	M	13:29	0:53	0.06	0.02	40.53	0.01	0.00
253	M	14:34	1:58	0.04	0.03	40.28	0.02	0.01
254	M	15:06	2:30	0.05	0.06	39.57	0.01	0.00
255	M	15:55	3:19	0.05	0.04	39.66	0.00	0.00
256	M		Backgrounc	0.05	0.04	40.01	0.00	0.00
257	M	13:03	0:27	0.08	0.03	40.60	0.00	0.00
258	M	13:16	0:40	0.05	0.02	40.38	0.01	0.00
259	M	13:29	0:53	0.03	0.01	64.06	0.01	0.01
260	M	14:34	1:58	0.05	0.04	68.95	0.01	0.00
261	M	15:06	2:30	0.09	0.01	66.04	0.00	0.00
262	M	15:55	3:19	0.04	0.04	62.21	0.01	0.00

Isotherm Data

Sample No.	Soil	Added Conc. (ppm)	Abs	Conc. (ppm)	P in Solution (ppm)	total P added (mg)	P in sol (mg)	P sorbed onto soil (mg/kg)
1	1	0		1.3	1.168	0	0.05256	-17.52
2	1	0		1.1	0.4642	0	0.020889	-6.963
3	1	0		1.3	0.3532	0	0.015894	-5.298
4	1	0		0.1	0.1003	0	0.004514	
5	1	1		1.2	1.22	0.039	0.0549	-5.3
6	1	1		1	1.214	0.039	0.05463	-5.21
7	1	1		0.7	1.264	0.039	0.05688	-5.96
8	1	1		1.1	0.884	0.039	0.03978	
9	1	5		1.2	2.915	0.0207	0.131175	-36.825
10	1	5		1.8	2.964	0.0207	0.13338	-37.56
11	1	5		2.1	3.529	0.0207	0.158805	-46.035
12	1	5		5	4.617	0.0207	0.207765	
13	1	10		9.4	7.12	0.448	0.3204	42.533333
14	1	10		8.1	8.04	0.448	0.3618	28.733333
15	1	10		7.7	7.79	0.448	0.35055	32.483333
16	1	10		9.8	9.97	0.448	0.44865	
17	1	25		22.8	20.99	1.108	0.94455	54.483333
18	1	25		22.8	21.2	1.108	0.954	51.333333
19	1	25		22.6	20.45	1.108	0.92025	62.583333
20	1	25		27	24.64	1.108	1.1088	
21	1	50		42.5	45.01	2.277	2.02545	83.85
22	1	50		39.7	45.32	2.277	2.0394	79.2
23	1	50		48.4	45.36	2.277	2.0412	78.6
24	1	50		53.5	50.6	2.277	2.277	
25	1	100		102.8	93.2	4.49	4.194	98.666667
26	1	100		98.6	92.8	4.49	4.176	104.66667
27	1	100		101.4	94.6	4.49	4.257	77.666667
28	1	100		110.7	99.8	4.49	4.491	
29	1	200		203.9	189.1	9.0495	8.5095	180
30	1	200		208	192.5	9.0495	8.6625	129
31	1	200		197.3	189	9.0495	8.505	181.5
32	1	200		210.2	201.1	9.0495	9.0495	
33	1	400		408.7	392.1	18.212	17.6445	189.16667
34	1	400		422.2	381.9	18.212	17.1855	342.16667
35	1	400		413.4	398.9	18.212	17.9505	87.166667
36	1	400		434.5	404.7	18.212	18.2115	
37	1	800		854	806	36.667	36.27	132.33333
38	1	800		839	793	36.667	35.685	327.33333
39	1	800		844	798	36.667	35.91	252.33333
40	1	800		859	815	36.667	36.675	

Laboratory Flow-Through Experiment Data

High flow rate: 13.8 mL/min

Elapsed Time (min)	Inflow Concentration (ppm)	ICP P Concentration (ppm)	Ortho P Concentration (ppm)	Ca Concentration (ppm)
0	0	0.1	0.09	1.65
0	0	0.1	0.05	1.77
0	0	0.2	0.06	1.47
0	0	0.1	0.12	1.37
0	0	0.1	0.09	1.76
0	0	0.1	0.05	1.36
1	1	0.7	0.66	0.52
1	1	0.7	0.71	0.49
1	1	0.8	0.78	0.6
8	1	0.9	0.77	0.39
9	1	1.0	0.89	0.42
10	1	1.0	0.89	0.37
14	1	1.0	0.90	0.37
14	1	1.0	0.84	0.39
15	1	1.0	0.97	0.32
28	1	1.0	0.85	0.39
29	1	1.0	0.92	0.31
30	1	1.1	0.97	0.3
48	1	1.0	0.88	0.29
49	1	1.1	0.93	0.23
50	1	1.1	0.87	0.24
78	1	1.0	0.77	0.24
79	1	1.0	0.86	0.19
80	1	1.1	0.87	0.2
108	1	1.0	0.85	0.21
109	1	1.0	0.86	0.19
110	1	1.0	0.87	0.18
138	1	1.0	0.78	0.18
139	1	1.0	0.80	0.15
140	1	1.1	0.73	0.16
1	2	1.6	1.53	0.79
1	2	1.9	1.63	0.77
3	2	1.4	1.30	0.94
6	2	2.0	1.91	0.85
6	2	2.0	1.92	0.63
7	2	2.1	1.90	0.76
11	2	2.1	2.01	0.56
12	2	2.1	1.96	0.78
12	2	2.1	2.02	0.65
24	2	2.0	1.69	0.39
25	2	2.1	2.09	0.47
26	2	2.1	1.99	0.48
45	2	2.0	1.91	0.29
46	2	2.1	1.93	0.37
47	2	2.1	1.84	0.29
74	2	2.1	1.90	0.24
75	2	2.1	1.86	0.24
76	2	2.1	1.90	0.21
104	2	2.1	1.90	0.22
105	2	2.1	1.86	0.23
106	2	2.1	1.91	0.17
134	2	2.1	1.91	0.2
135	2	2.1	1.91	0.18
136	2	2.1	1.93	0.11

Low flow rate: 0.4 mL/min

Elapsed Time	Inflow Concentration (ppm)	Ca Concentration (ppm)	ICP P Concentration (ppm)
0:00	0	3.9	0.1
0:00	0	4.0	0.2
0:00	0	2.7	0.1
0:00	0	4.2	0.1
0:00	0	4.9	0.1
0:00	0	4.0	0.1
0:00	1.1	1.9	0.2
0:00	0.9	1.0	0.3
0:00	0.8	1.0	0.2
0:15	1.1	0.8	0.2
0:15	0.9	0.8	0.3
0:17	0.8	0.7	0.2
0:30	1.1	0.7	0.2
0:30	0.9	0.7	0.3
0:32	0.8	0.6	0.3
0:45	1.1	0.7	0.3
0:45	0.9	0.7	0.4
0:47	0.8	0.6	0.3
1:01	1.1	0.7	0.3
1:01	0.9	0.7	0.5
1:02	0.8	0.6	0.4
1:19	1.1	0.7	0.5
1:19	0.9	0.7	0.3
1:17	0.8	0.6	0.4
1:31	0.8	0.7	0.5
1:34	1.1	0.7	0.4
1:34	0.9	0.7	0.5
2:03	0.8	0.7	0.5
2:04	1.1	0.6	0.4
2:04	0.9	0.8	0.5
2:35	1.1	0.6	0.4
2:35	0.9	0.7	0.6
2:33	0.8	0.7	0.6
3:05	1.1	0.5	0.4
3:05	0.9	0.7	0.6
3:05	0.8	0.7	0.6
3:35	1.1	0.5	0.5
3:35	0.9	0.7	0.7
3:38	0.8	0.6	0.6
4:05	1.1	0.5	0.5
4:05	0.9	0.7	0.7
4:08	0.8	0.7	0.7
4:35	1.1	0.5	0.5
4:35	0.9	0.8	0.8
4:38	0.8	0.6	0.7
5:05	1.1	0.5	0.5
5:05	0.9	0.7	0.7
5:08	0.8	0.7	0.7
5:35	1.1	0.5	0.5
5:35	0.9	0.7	0.8
5:38	0.8	0.6	0.7
6:05	1.1	0.5	0.5
6:05	0.9	0.7	0.8
6:08	0.8	0.6	0.7

6:35	1.1	0.5	0.6
6:35	0.9	0.7	0.8
6:38	0.8	0.6	0.8
7:05	1.1	0.5	0.6
7:05	0.9	0.7	0.8
7:08	0.8	0.6	0.7
7:35	1.1	0.5	0.6
7:35	0.9	0.7	0.9
7:38	0.8	0.6	0.7
8:05	1.1	0.5	0.6
8:05	0.9	0.6	0.8
8:08	0.8	0.6	0.7
0:00	1.6	1.3	0.5
0:00	1.6	1.4	0.3
0:00	1.5	1.0	0.4
0:15	1.5	0.9	0.5
0:12	1.6	0.9	0.3
0:17	1.6	0.8	0.4
0:27	1.6	0.8	0.4
0:30	1.5	0.9	0.6
0:32	1.6	0.7	0.4
0:42	1.6	0.8	0.5
0:45	1.5	0.8	0.7
0:47	1.6	0.7	0.5
0:57	1.6	0.9	0.7
1:00	1.5	0.9	0.8
1:02	1.6	0.8	0.6
1:12	1.6	0.9	0.8
1:15	1.5	0.9	0.9
1:17	1.6	0.8	0.7
1:26	1.6	0.9	0.8
1:29	1.5	0.9	1.0
1:31	1.6	0.8	0.7
1:58	1.6	1.0	1.1
2:01	1.5	0.9	1.0
2:03	1.6	0.9	1.0
2:28	1.6	1.1	1.3
2:31	1.5	0.9	1.1
2:33	1.6	0.9	1.2
3:00	1.6	1.0	1.4
3:03	1.5	0.9	1.2
3:05	1.6	0.9	1.3
3:33	1.6	1.0	1.4
3:36	1.5	0.9	1.2
3:38	1.6	0.9	1.3
4:03	1.6	1.0	1.4
4:06	1.5	0.9	1.3
4:08	1.6	0.9	1.3
4:33	1.6	1.0	1.4
4:36	1.5	0.9	1.3
4:38	1.6	0.9	1.4
5:03	1.6	1.0	1.5
5:06	1.5	0.9	1.4
5:08	1.6	0.8	1.4
5:33	1.6	1.0	1.5
5:36	1.5	0.9	1.4
5:38	1.6	0.8	1.4
6:03	1.6	0.9	1.5
6:06	1.5	0.9	1.4
6:08	1.6	0.8	1.4
6:33	1.6	0.9	1.5
6:36	1.5	0.9	1.4
6:38	1.6	0.8	1.5
7:03	1.6	0.9	1.6
7:06	1.5	0.8	1.4
7:08	1.6	0.8	1.5
7:33	1.6	0.9	1.6
7:36	1.5	0.8	1.5
7:38	1.6	0.8	1.5
8:03	1.6	0.8	1.6
8:06	1.5	0.8	1.4
8:08	1.6	0.7	1.4

VITA

John William Fuchs

Candidate for the Degree of

Master of Science

Thesis: Subsurface Transport of Phosphorus in Riparian Floodplains: Tracer and Phosphorus Transport Experiments

Major Field: Biosystems and Agricultural Engineering

Biographical:

Personal Data: Born February 4, 1984 in Cape Girardeau, MO, the son of John and Nora Fuchs

Education: Completed the requirements for the Master of Science in Biosystems and Agricultural Engineering at Oklahoma State University, Stillwater, Oklahoma in May, 2008.
Completed the requirements for the Bachelor of Science in Civil Engineering at the University of Mississippi, Oxford, Mississippi in May, 2006.

Experience: Undergraduate research assistant, University of Mississippi, Oxford, Mississippi, June 2005 – May 2006.
Graduate research assistant, Oklahoma State University, Stillwater, Oklahoma, August 2006 – present.

Professional Memberships: American Society of Agricultural and Biological Engineers (ASABE), American Society of Civil Engineers (ASCE), Chi Epsilon, National Society for Collegiate Scholars

Name: John William Fuchs Date of Degree: May 2008

Institution: Oklahoma State University Location: Stillwater, Oklahoma

Title of Study: Subsurface Transport of Phosphorus in Riparian Floodplains: Tracer and Phosphorus Transport Experiments

Pages in Study: 51 Candidate for the Degree of Master of Science

Major Field: Biosystems and Agricultural Engineering

Scope and Method of Study: The primary transport mechanism for phosphorus (P) movement from upland areas to surface water systems is typically surface runoff, with subsurface transport assumed negligible. However, certain local conditions can lead to an environment where subsurface transport may be significant. The objective of this research was to determine the importance of subsurface transport of P along streams characterized by cherty or gravel subsoils. At a field site adjacent to the Baron Fork Creek, a trench was installed with the bottom of the trench at topsoil/alluvial gravel interface. Fifteen piezometers were installed at various locations surrounding the trench in order to monitor flow and transport. In three separate experiments, water was pumped into the trench from the Baron Fork Creek to maintain a constant head. At the same time, a conservative tracer (Rhodamine WT) and/or potassium phosphate were injected into the trench at concentrations ranging between 3 and 100 ppm for Rhodamine WT and at 100 ppm for P. Laboratory flow cell experiments were also conducted to determine the effect that flow velocity had on P sorption.

Findings and Conclusions: Rhodamine WT and P were detected in some piezometers at equivalent concentrations as measured in the trench, suggesting the presence of preferential flow pathways. Phosphorus sorption was minimal ($R = 1$, where R is the retardation coefficient) along the preferential flow pathways but transport was retarded in non-preferential flow paths ($R > 5$ to 6). The effect that flow velocity has on P sorption was tested in the laboratory using flow through cells. Results suggested that velocity did have an effect on P sorption of the alluvial subsoil. The potential for nutrient transport shown by this alluvial system has implications regarding alternative management of similar riparian floodplain systems.

ADVISER'S APPROVAL: Dr. Garey A. Fox